Authors: Ken Stewart Brian Hicks	Date of issue: 2003-11-26 Kind of issue: confidential	Scope: lofar/engineering Doc.id: NRL Status Report
	Status: final Revision nr: 1	

LOFAR NRL Alternative Low-Band Antenna and Balun Designs
Progress Report
November 26, 2003

Verified:			
Name	Signature	Date	Rev.nr.
Ken Stewart Brian Hicks		2004-01-13 2004-01-13	1.0 1.0

Accepted:		
SEG	PMT	ISC

Distribution list:

Group:	For Information:
SEG PMT ISC WPM	TAC

Document history:

Revision	Date	Section	Page(s)	Modification
0.5	2003-11-26		-	First draft
1.0	2004-1-13			Release version
1.1	2004-1-21	4.5, 4.6		Revised CLRO, Sinuous antenna comments
1.2	2004-1-22	4.7	33	Table 2

1.1 Table of contents:

2 Introduction

2.1 Purpose of this document

This document summarizes the work done at NRL on alternative low band antenna and active balun designs. We evaluate several possible alternatives to see how well they meet the LOFAR specifications and compare them with the inverted-V active dipole baseline design.

2.2 Development philosophy

2.3 Applicable documents

LOFAR-ASTRON-SRS-001: LOFAR System Requirements Specification
LOFAR-ASTRON-PLN-007: LOFAR Design, Development & Verification Plan
LOFAR-ASTRON-ADD-006: LOFAR Architectural Design Document
LOFAR-ASTRON-RPT-002: LOFAR Glossary

2.4 Definitions

In addition to the current version of the LOFAR Glossary, the following definitions are used:
HBA: High Band Antenna(120-250 MHz)
HPBW: Half-Power Beam Width
LBH: Low Band High (30-90 MHz)
LBL: Low Band Low (10-40 MHz)
VSWR: Voltage Standing Wave Ratio

3 Active Balun Development

3.1 NLTA Test Balun

The NRL Test Balun is a highly linear, low noise preamplifier designed to assist in the characterization of antenna topologies. It has a 1dB compression point at 24.9 dBm (output power), a gain of 33.4 dB, and a noise figure of 3.77 dB. It uses amplifiers intended for the cable TV industry, and would be prohibitively expensive, at ~$200 per unit, to use in the final LOFAR application.

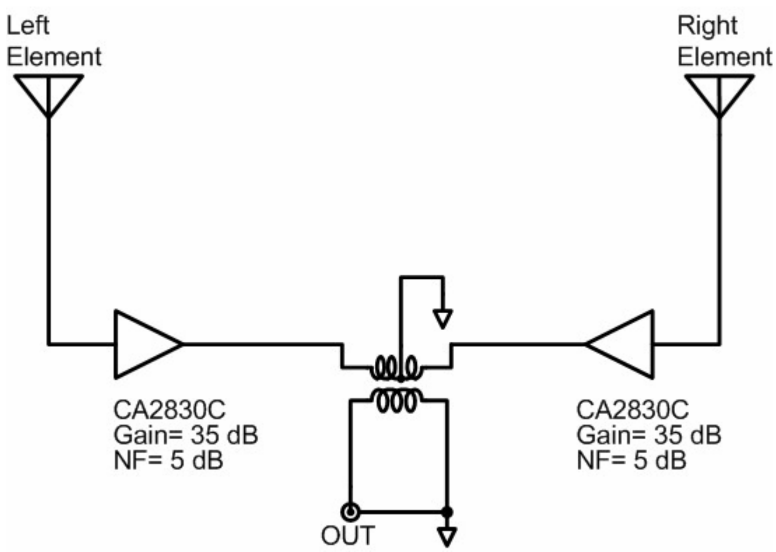

Figure 1. Simplified schematic of NLTA active balun.

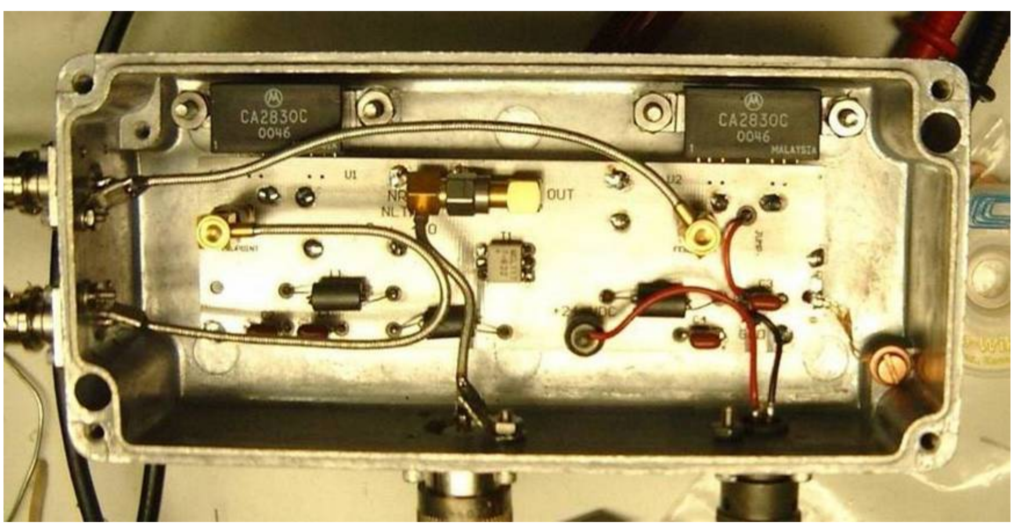

Figure 2. Prototype implementation of NLTA active balun.

3.2 Test Measurements of NLTA Balun

Figure 3 shows a galactic background spectrum observed with one of the NLTA dipoles plus a 50 MHz lowpass filter to attenuate the VHF commercial broadcast stations. The lowest trace is the system noise with the active balun switched off. The middle trace (nearly on top of the first trace on this scale) was made with a 50 Ω load substituted for the dipole. This spectrum shows the thermal noise of the load (290 K) plus the excess noise generated by the preamp (387 K). The top trace shows the spectrum with the dipole connected and observing the sky (both galactic and terrestrial noise). The slope of the curve is consistent with the $v^{-2.55}$ dependence of the galactic brightness temperature at these frequencies (Cane 1979).

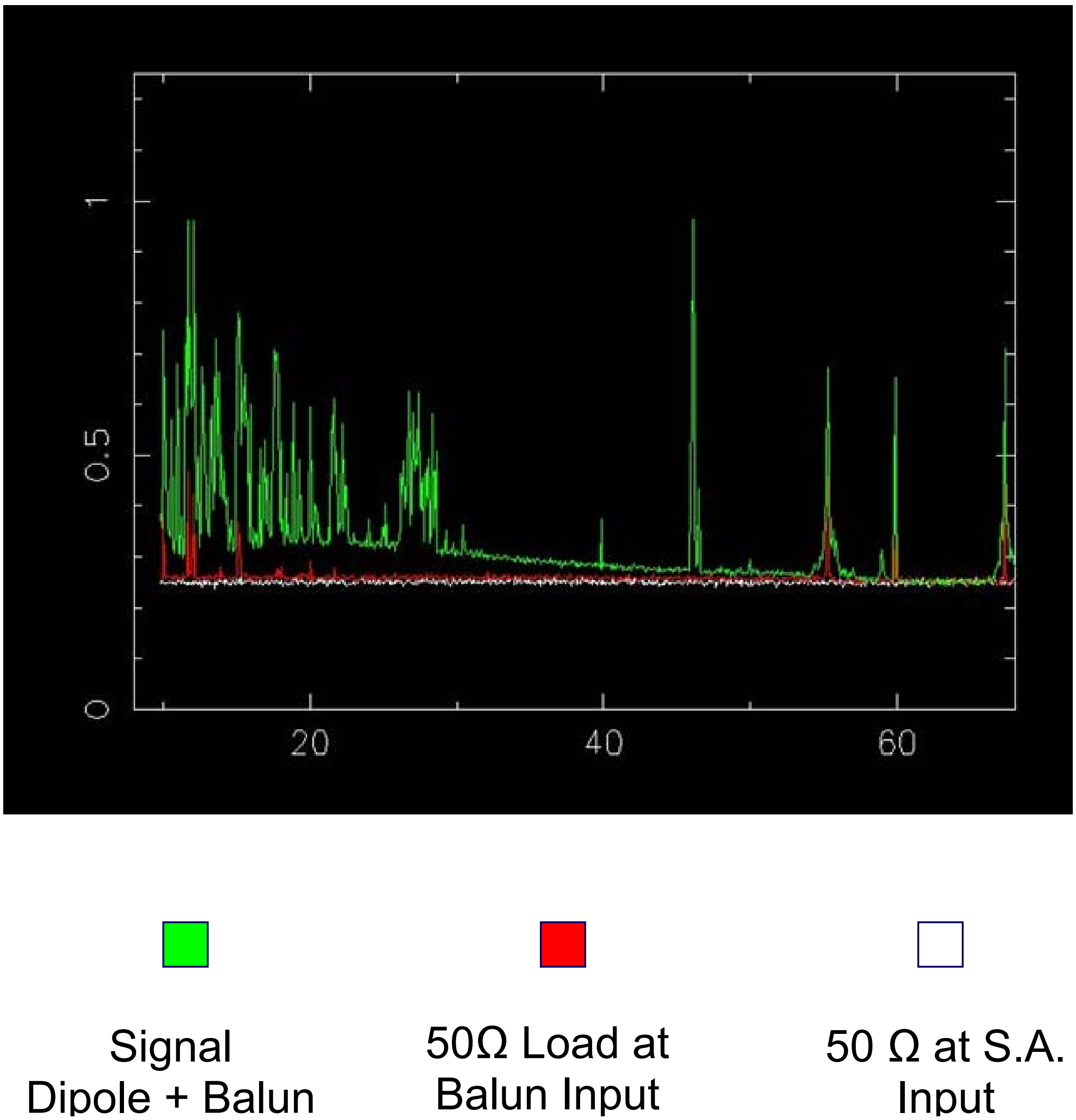

Figure 3. Measurements taken at the NRL Low-Frequency Test Array (NLTA), with the slope of the galactic background clearly visible.

3.3 ASTRON Baseline Active Balun Design

The ASTRON active-balun is a transimpedance amplifier based on commercially available components that is approaching the cost and performance requirements for LOFAR. At 40 MHz it delivers a gain of 12.7 dB, with a 1 dB compression point of 11.6 dBm (output), and a third-order intercept at 28 dBm (output). It consumes only 1.5 W of power. This balun design is presently being manufactured for use in the Initial Test Station (10 – 40 MHz) and the THETA project (40 – 80 MHz).

3.4 NRAO/NRL Active Prototype Active Balun Design

The NRAO balun was initially developed for solar science applications. The schematic diagram (figure 4) and picture (figure 5) below represent an individual gain block in the NRAO/NRL active balun design. It has a nominal gain of 16 dB, with a 1dB compression point at 19.1 dBm (output) and third-order intercept at 32 dBm (output). It is also a transimpedance amplifier, and has power requirement of 0.65 W.

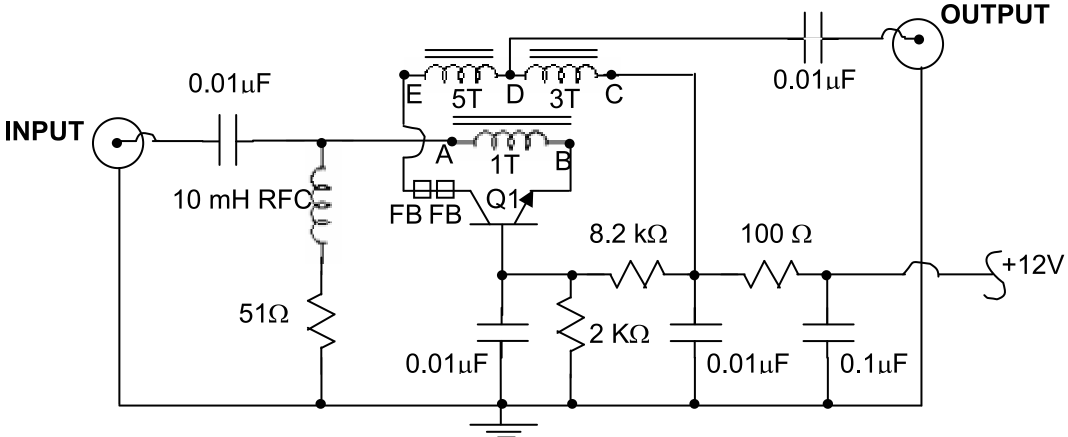

Figure 4. Schematic diagram of a gain block.

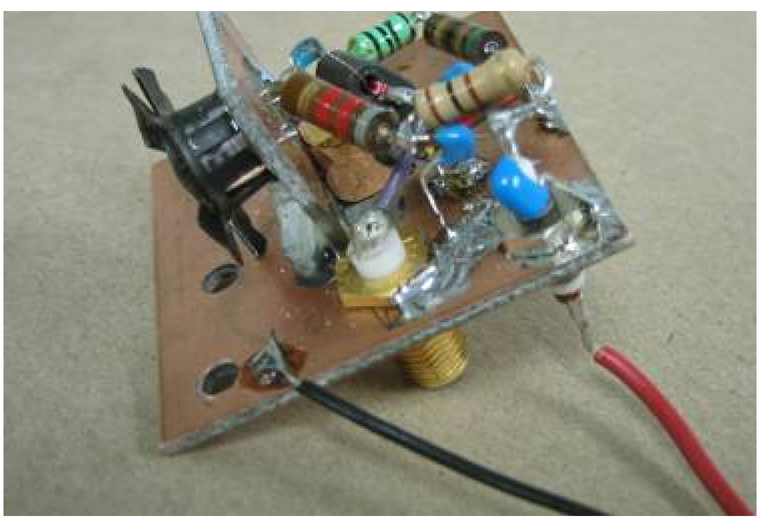

Figure 5. Working prototype gain block.

The NRAO balun shares the same basic topology as the all of the present balun candidates, with a 180° Hybrid being used instead of a transformer throughout the initial development. The hybrid will be replaced with a low cost transformer in the final design, which is presently being refined to also increase the system gain. The noise temperature of the NRAO design has been measured at 175 K.

The present development plan for this balun will result in a device that will have 50 Ω output impedance, and require that power be supplied via separate cabling. We believe that it may be possible to achieve a better output impedance match with this method, and are pursuing such designs to determine if the difference is significant enough to warrant the additional cabling cost. The ASTRON baseline design requires DC power through the same coaxial cable used to deliver the signal from the output.

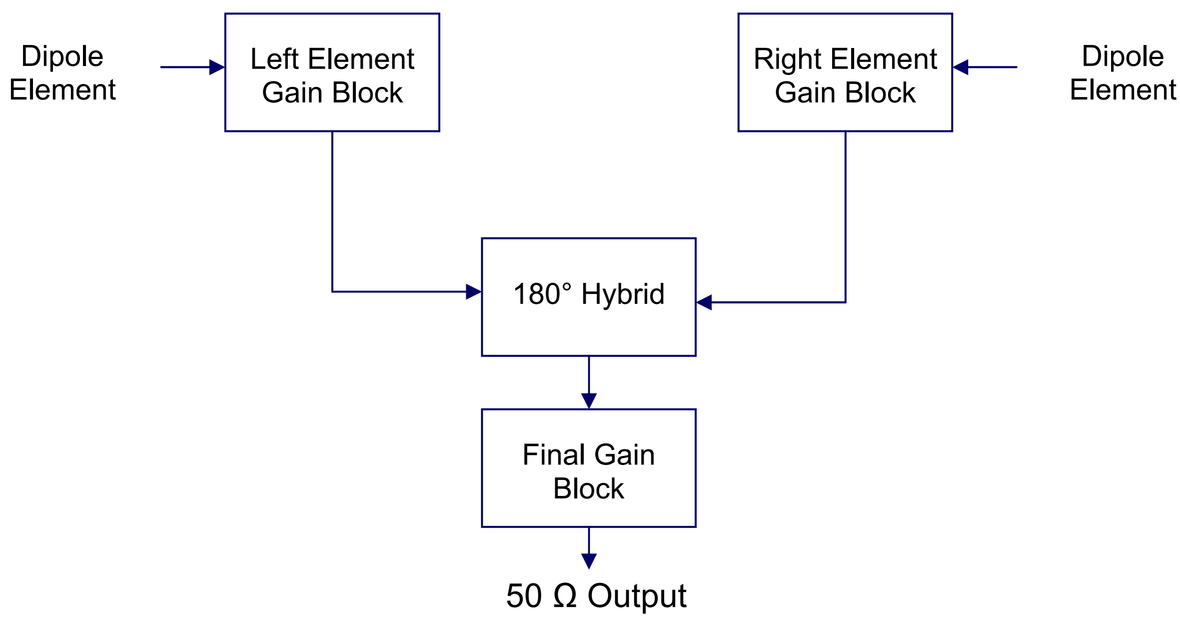

Figure 6. Block diagram of NRAO active-balun.

3.5 Summary of LFA Balun Requirements and Progress

The table below summarizes the performance of the present balun designs.

There has been considerable progress in active-balun development since the PDR, and this is reflected in the fact that all of the values given here have been taken from working prototypes at three cooperating institutions. It is expected that the experience gained in the development of each of these devices will soon result in a final design that incorporates the strengths of all of them.

Balun designs with a high input impedance are still under consideration at NRL, and we may explore the potential for their use further in the near future.

Table 1. Summary of LFA Balun Development – Requirements and Progress

Specification	Target	Baseline Design (ASTRON)	Transimpedance (NRAO)	NLTA Test Balun (NRL)
Gain	Unspecified	12.7 dB (40 MHz)	16 dB	33.4 dB
Noise Temperature	Less than 10% of sky noise power	TBD	175 K	386.9 K
1 dB Compression Point	Unspecified	11.6 dBm (40MHz)	19.1 dBm (Output)	24.9 dBm (Output)
IP2	> +38 dBm (TBD)	41 dBm (40 MHz)	58.5 dBm (Output)	72 dBm (Output)
IP3	> +18 dBm (TBD)	28 dBm (40 MHz)	33.5 dBm (Output)	42 dBm (Output)
Output Impedance	75 Ω	~110 Ω	50 Ω	50 Ω
Power Required	TBD, minimal	1.5 W	0.65 W	14.4 W

4 Antenna Simulations and Comparisons

4.1 Antenna Designs: Introduction

Two different software packages were used to produce the numerical antenna response patterns and VSWR simulations shown in this section. The public domain NEC-2 Fortran code, which runs in a few seconds, was used for the wire antennas. CST Microwave Studio was used for more complex antennas, and to check some of the NEC-2 results, but these calculations usually require several hours of computer time.

4.2 ASTRON LBL baseline design

Figure 7 through Figure 15 show the NEC-2 simulations of the baseline LBL active antenna design. The arms of the dipole are 2.0 m long inclined 45º below horizontal. The feedpoint is 2.0 m above a 4 m × 4 m ground screen consisting of a mesh of orthogonal wires 10 cm apart. An infinite ground plane consisting of average soil (Table 2) is assumed underneath the mesh ground screen. These are dual polarized antennas with two dipoles 90° apart about the vertical axis. Only one of the dipoles is stimulated in these simulations, but the other wires are included in the model so that their minor effects on the response pattern are accounted for. Calculations for the 10 – 90 MHz LB frequency range are shown even though these antennas are intended to be used only below 40 MHz.

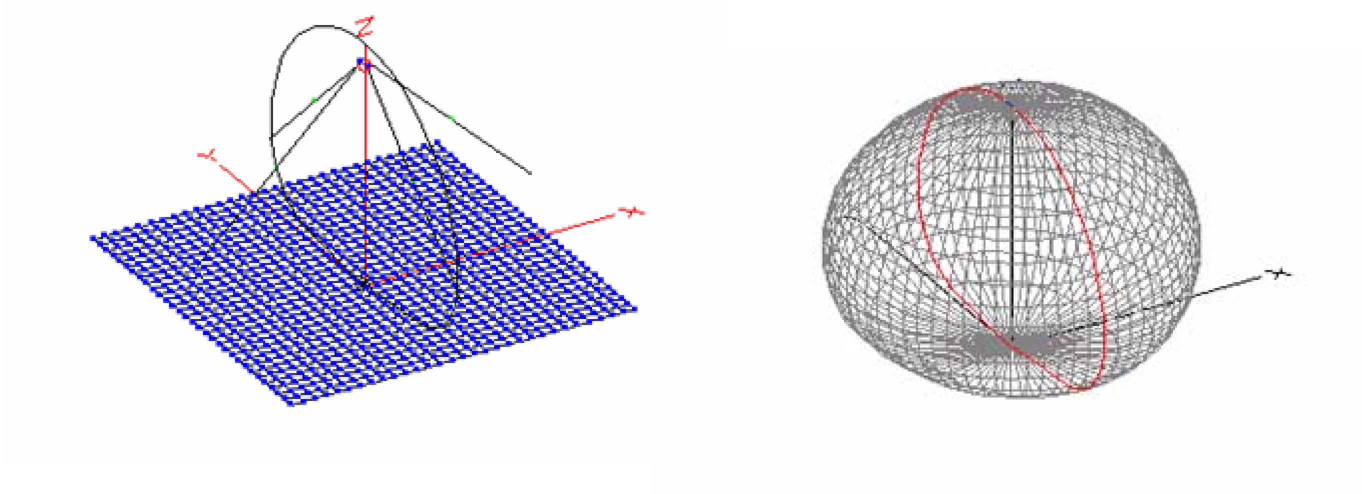

Figure 7. ASTRON LBL dipole (baseline design), 10 MHz: HPBW = 90° E-plane, 101° H-plane.

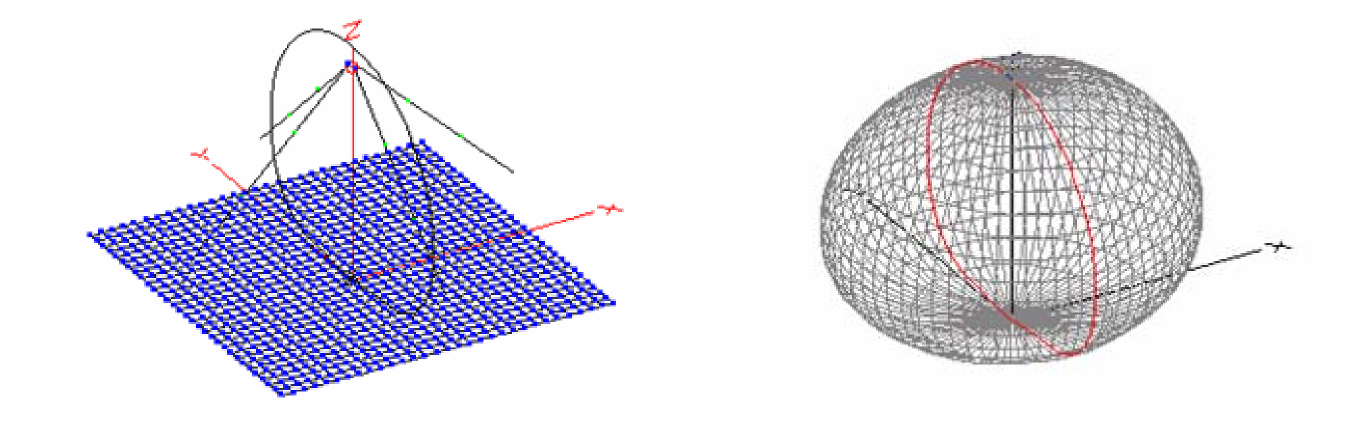

Figure 8. ASTRON LBL dipole (baseline design), 20 MHz: HPBW = 79° E-plane, 107° H-plane.

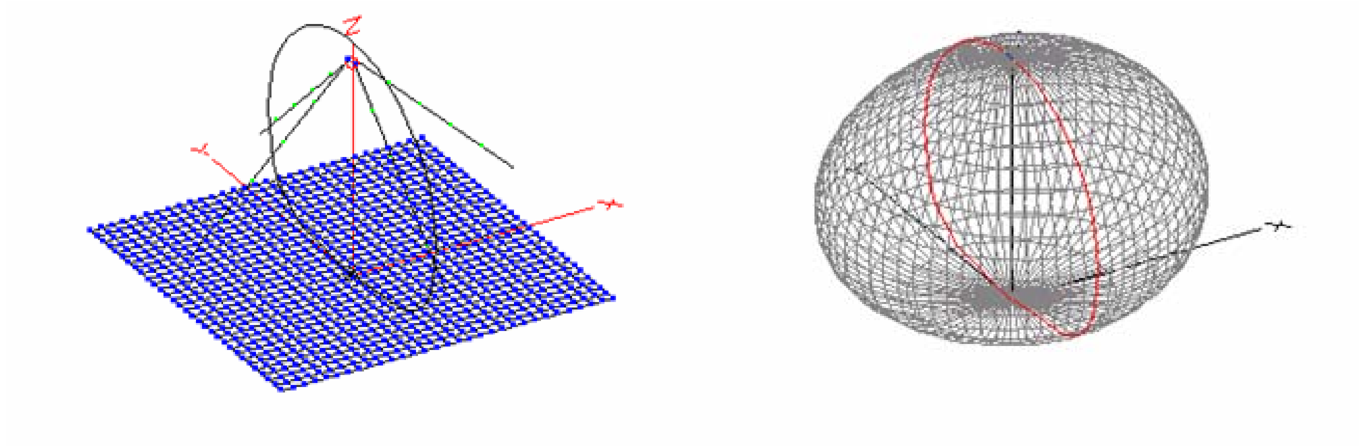

Figure 9. ASTRON LBL dipole (baseline design), 30 MHz: HPBW = 82° E-plane, 113° H-plane.

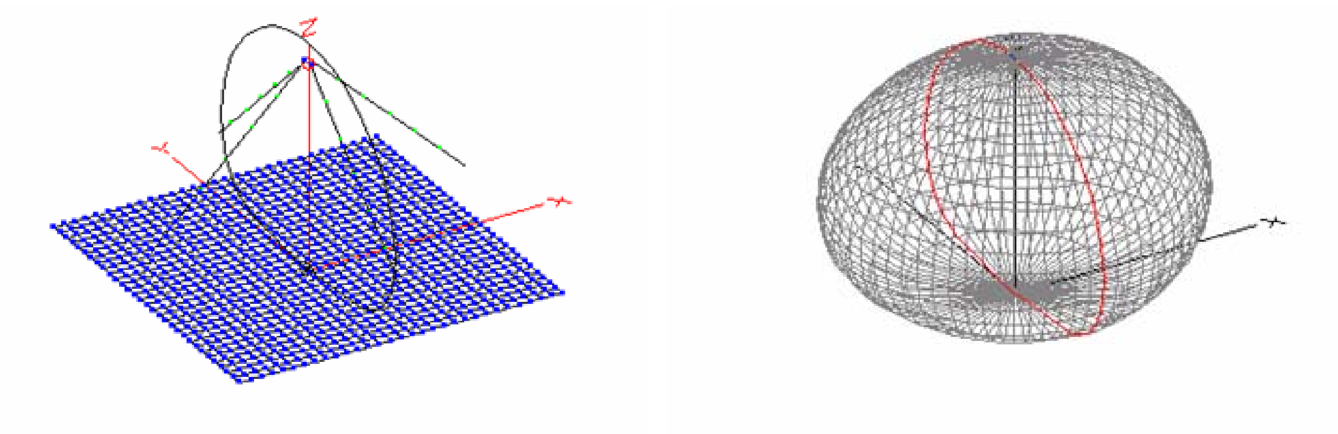

Figure 10. ASTRON LBL dipole (baseline design), 40 MHz: HPBW = 90° E-plane, 118° H-plane.

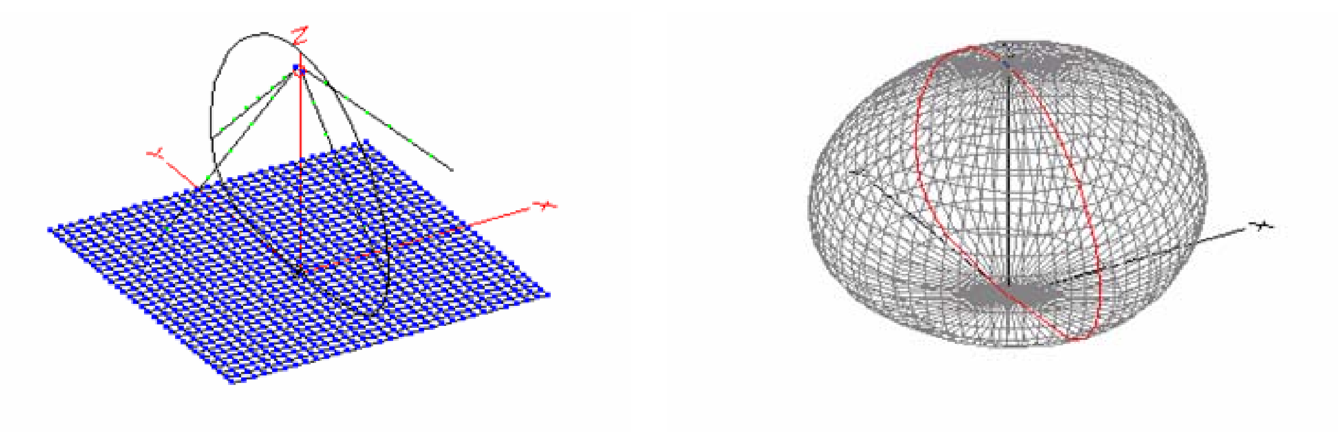

Figure 11. ASTRON LBL dipole (baseline design), 50 MHz: HPBW = 96° E-plane, 124° H-plane.

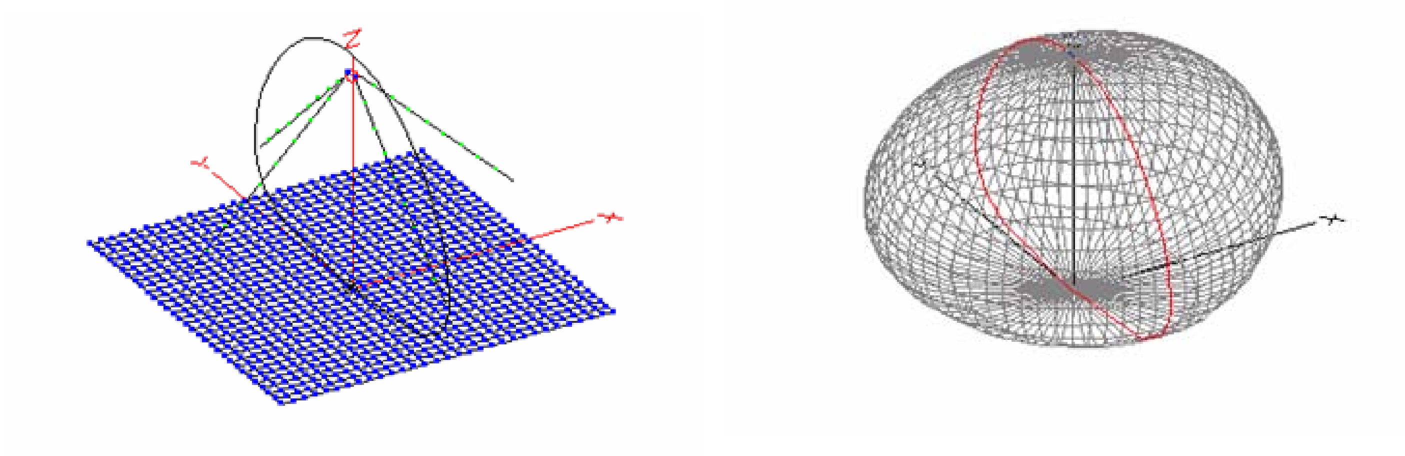

Figure 12. ASTRON LBL dipole (baseline design), 60 MHz: HPBW = 97° E-plane, 129° H-plane.

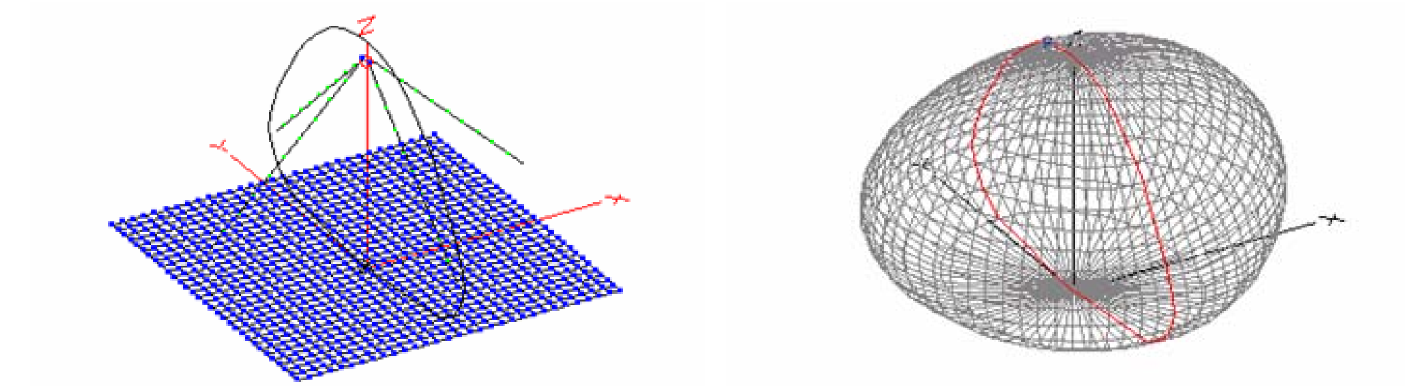

Figure 13. ASTRON LBL dipole (baseline design), 70 MHz: HPBW = 82° E-plane, 133° H-plane.

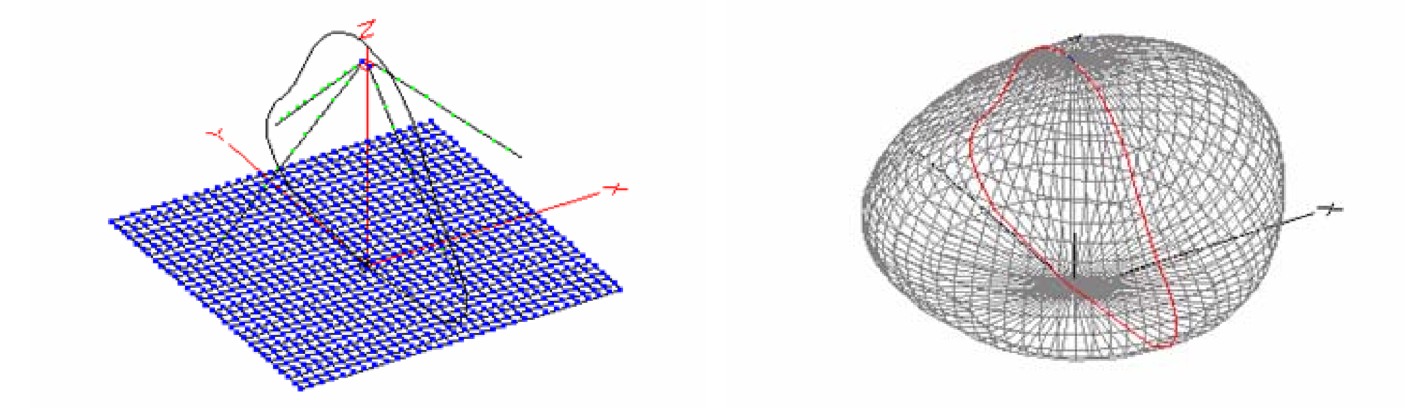

Figure 14. ASTRON LBL dipole (baseline design), 80 MHz: HPBW = 59° E-plane, 133° H-plane.

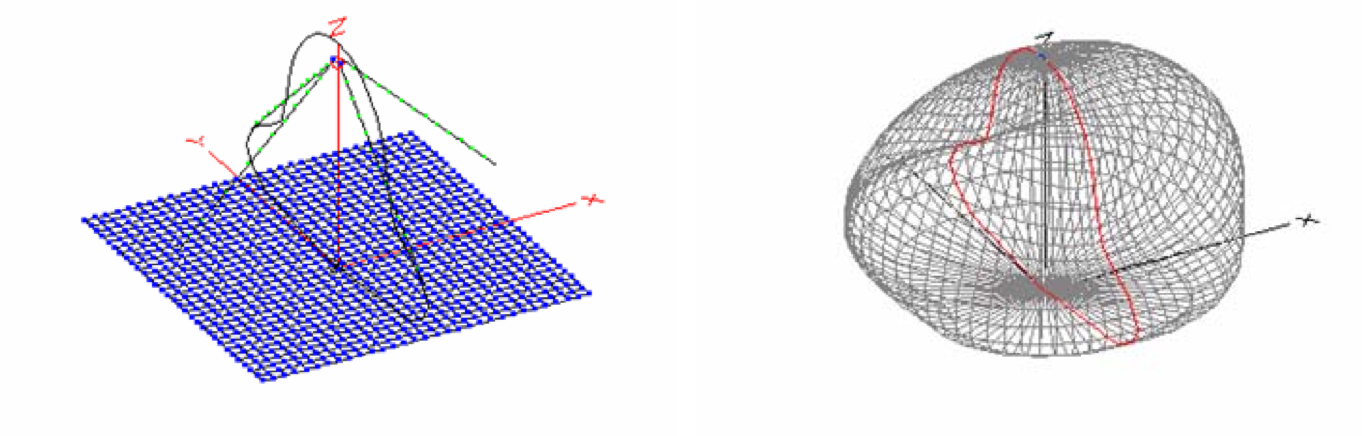

Figure 15. ASTRON LBL dipole (baseline design), 90 MHz: HPBW = 45° E-plane, 125° H-plane.

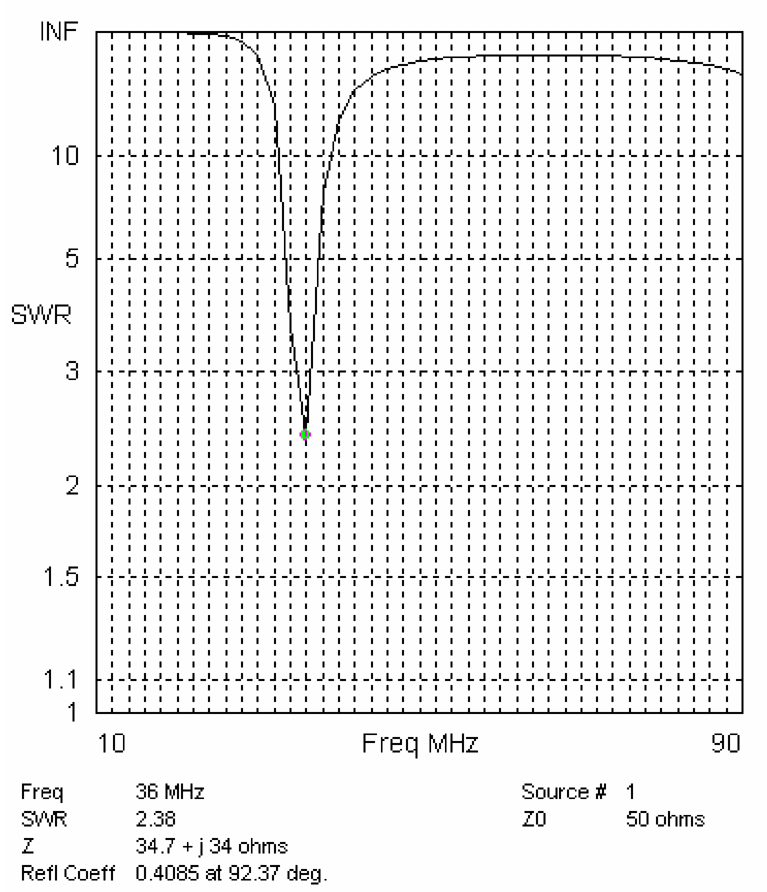

Figure 16. VSWR of baseline dipole in a 50 Ω feed line.

4.3 NLTA Inverted V-dipole

Figure 17 shows the development steps leading to the present NLTA design. A dipole made with thin wires (a), has narrow resonances when its length is an odd multiple of half the wavelength. Thicker wires cause the resonances to be broadened because the feedpoint impedance varies less and more slowly with frequency. A "cage" dipole (b) approximates a dipole constructed from very thick solid wires and therefore has less extreme impedance variations and better VSWR in the feedline, but is fragile and difficult to build. A simpler, planar design (c), with only three wires, is much easier to build and does not degrade the performance much compared with a six or eight wire cage design.

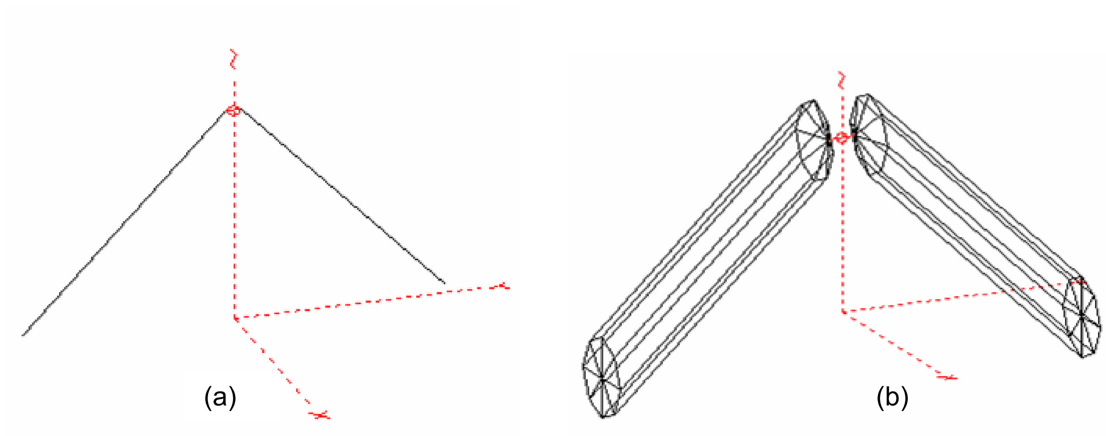

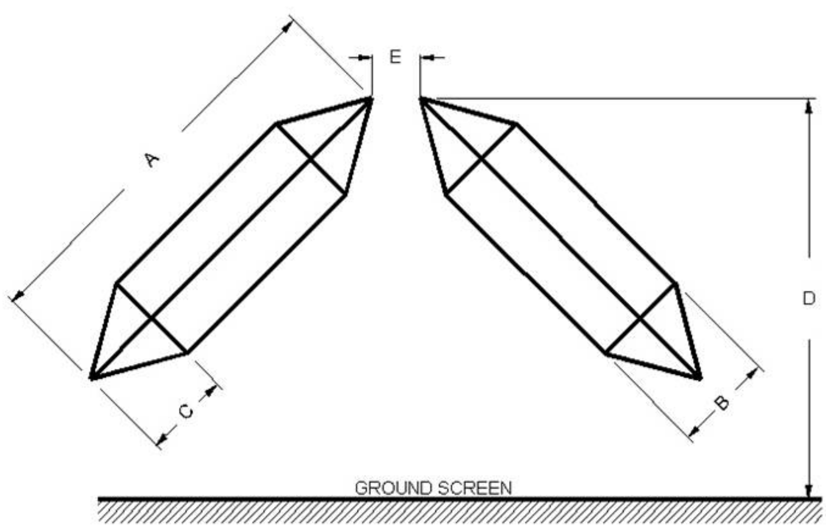

Dimensions (m)	*A*	*B*	*C*	*D*	*E*
Small dipole	1.20	0.30	0.26	1.32	0.06
Large dipole	3.24	1.00	0.87	3.48	0.06

(c)

Figure 17. Successive steps leading to the present NLTA design.

Further simulations showed that removing the end triangles from the structure in Figure 17(c) had negligible effect and permitted another simplification. The exact dimensions of the final design were determined by the ready availability of 6 ft (1.83 m) lengths of 15.8 mm diameter Cu tubing. Each arm was made from exactly four of these tubes. This was convenient for the rapid, hand construction of about 20 dipole arms needed for the eight-element test array plus spares.

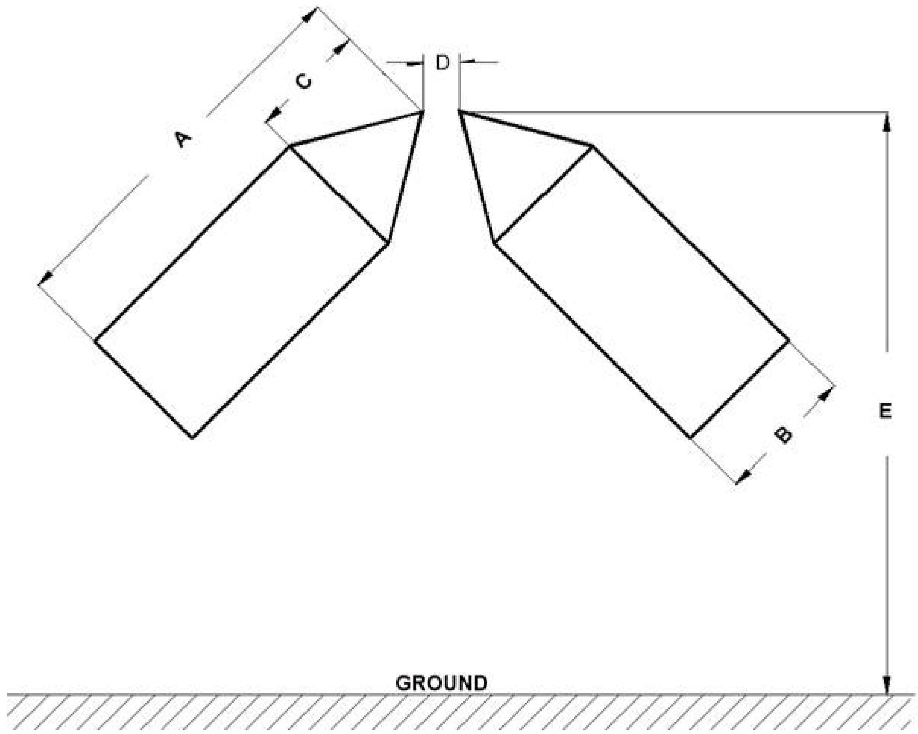

Dimensions (m)	A	B	C	D	E
	2.64	0.94	0.79	0.20	3.00

Figure 18. Details of the NLTA antenna design.

The NLTA antenna response patterns are shown in Figure 19 through Figure 27. Compared with the LOFAR baseline design, the pattern develops deeper nulls and stronger sidelobes at the high frequencies due to its larger size and greater height above ground.

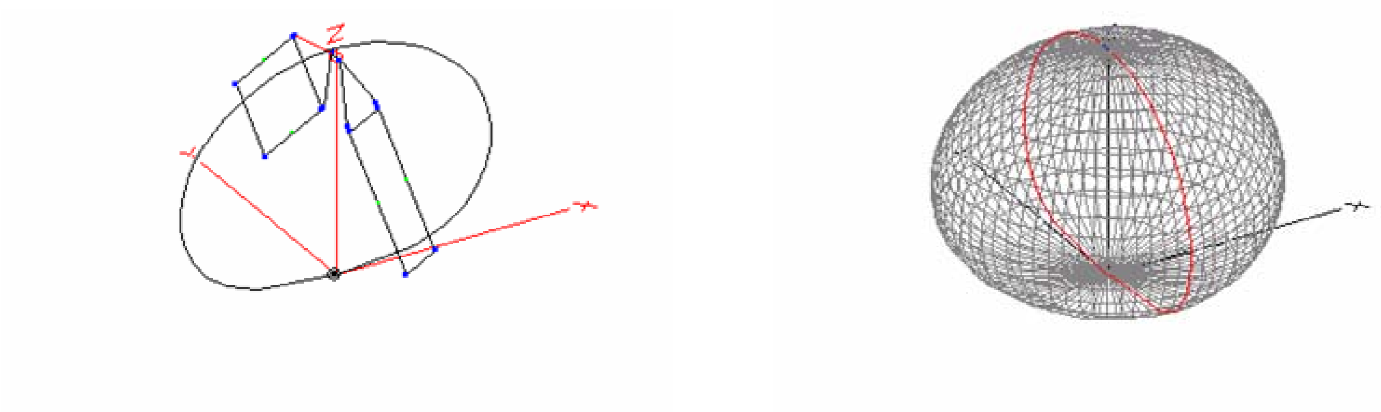

Figure 19. NLTA dipole, 10 MHz: HPBW = 84° E-plane, 102° H-plane.

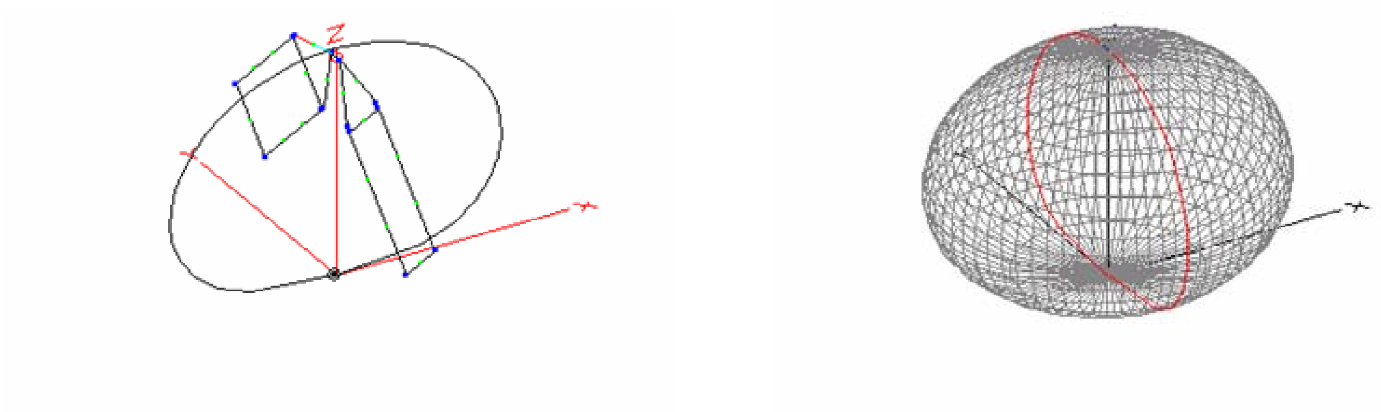

Figure 20. NLTA dipole, 20 MHz: HPBW = 81° E-plane, 114° H-plane.

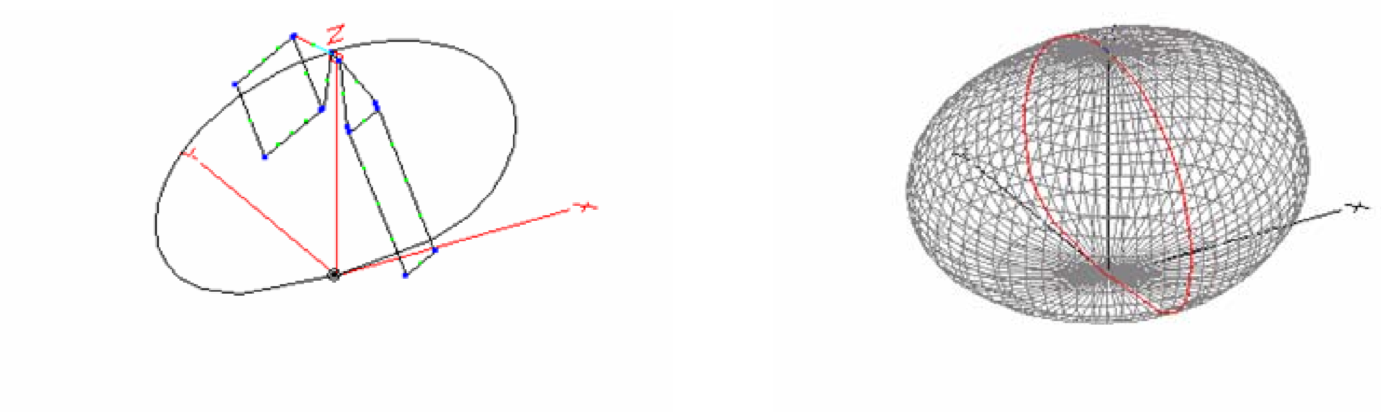

Figure 21. NLTA dipole, 30 MHz: HPBW = 84° E-plane, 130° H-plane.

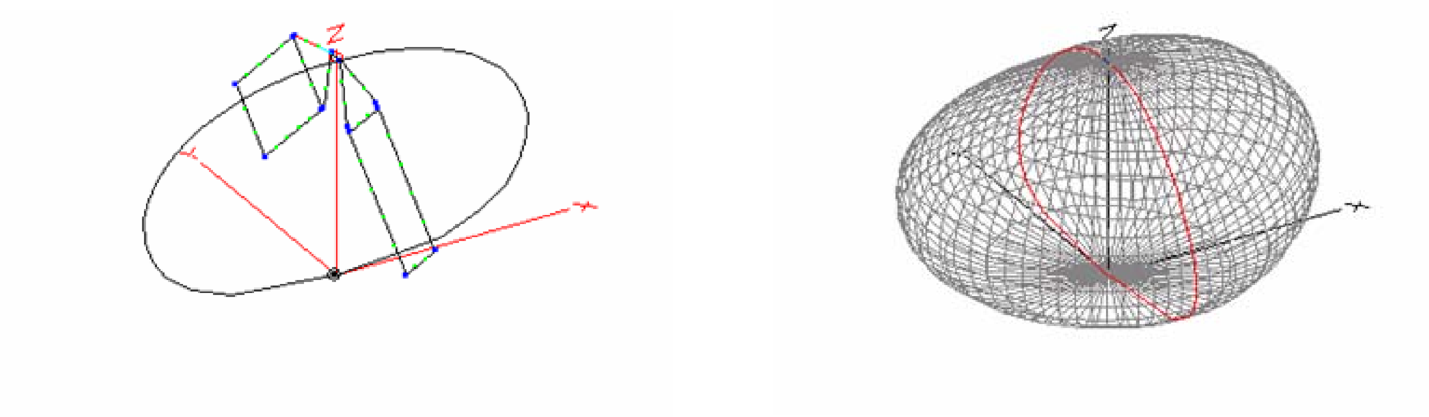

Figure 22. NLTA dipole, 40 MHz: HPBW = 87° E-plane, 139° H-plane.

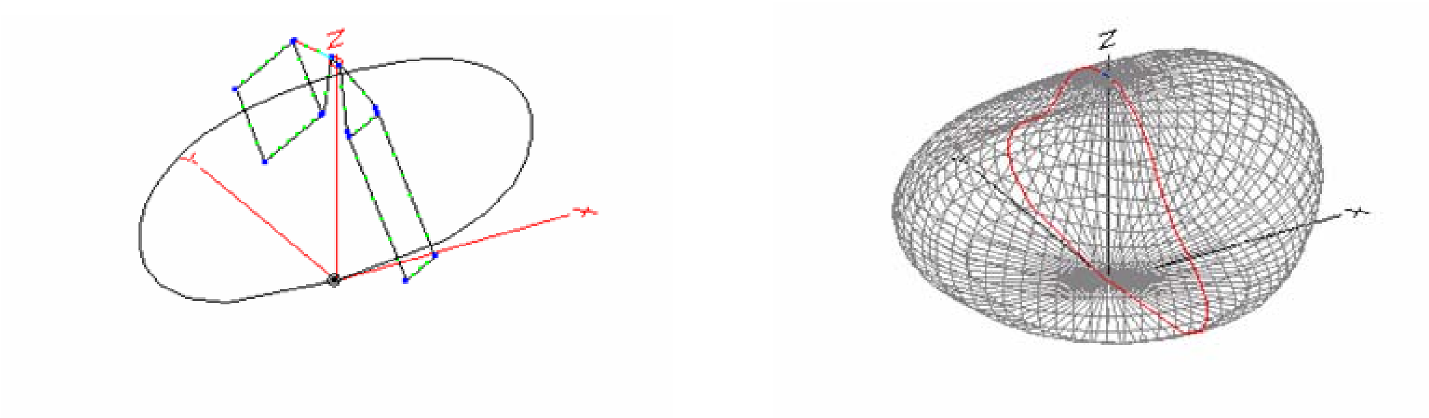

Figure 23. NLTA dipole, 50 MHz: HPBW = 53° E-plane, 143° H-plane.

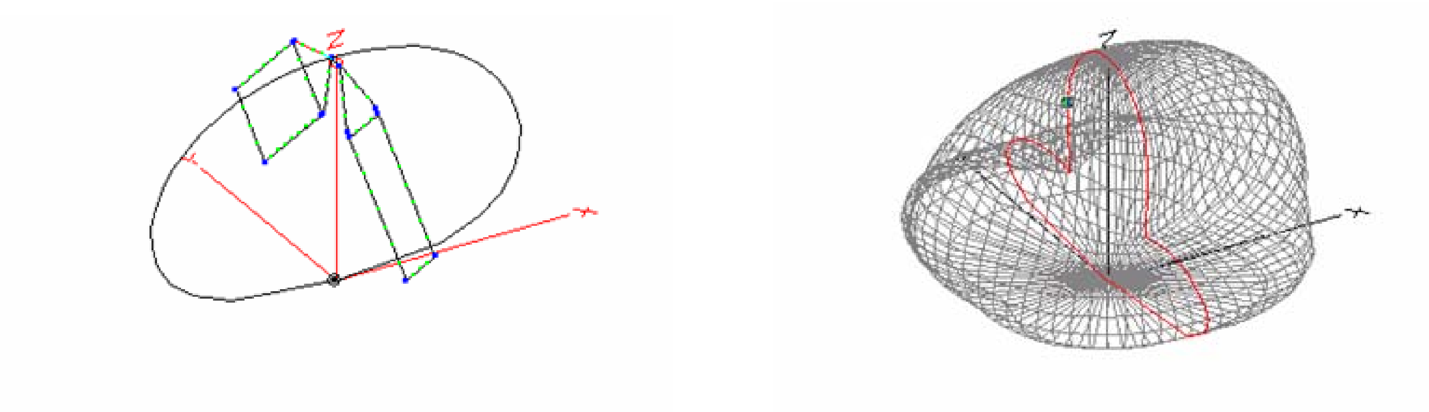

Figure 24. NLTA dipole, 60 MHz: HPBW = 37° E-plane, 135° H-plane.

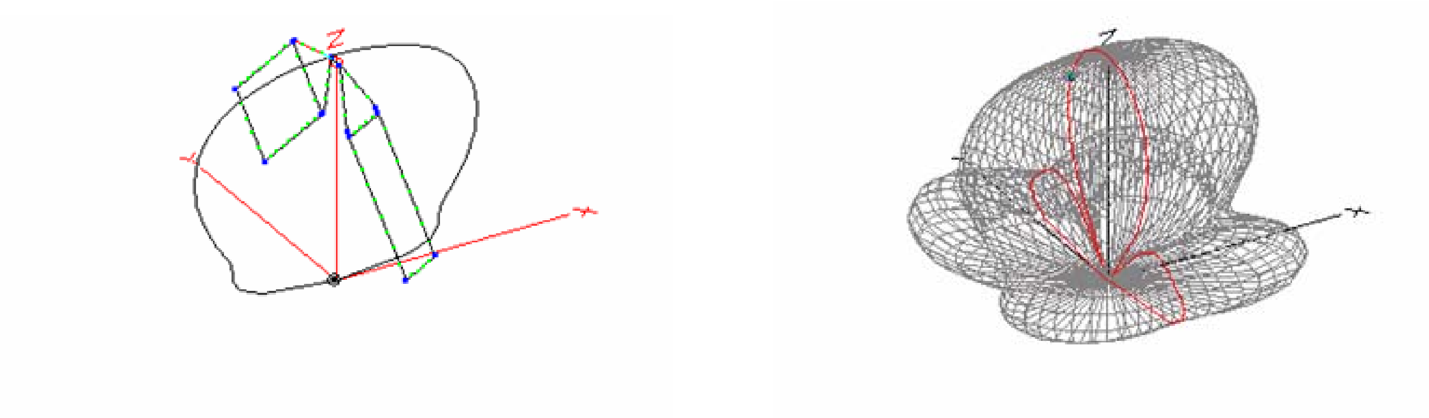

Figure 25. NLTA dipole, 70 MHz: HPBW = 37° E-plane, 92° H-plane.

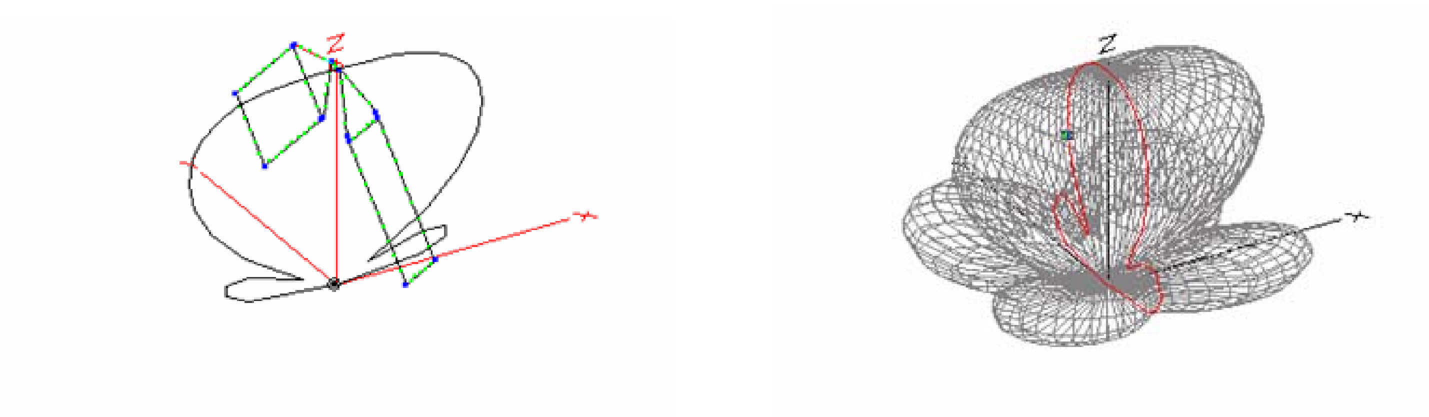

Figure 26. NLTA dipole, 80 MHz: HPBW = 40° E-plane, 94° H-plane.

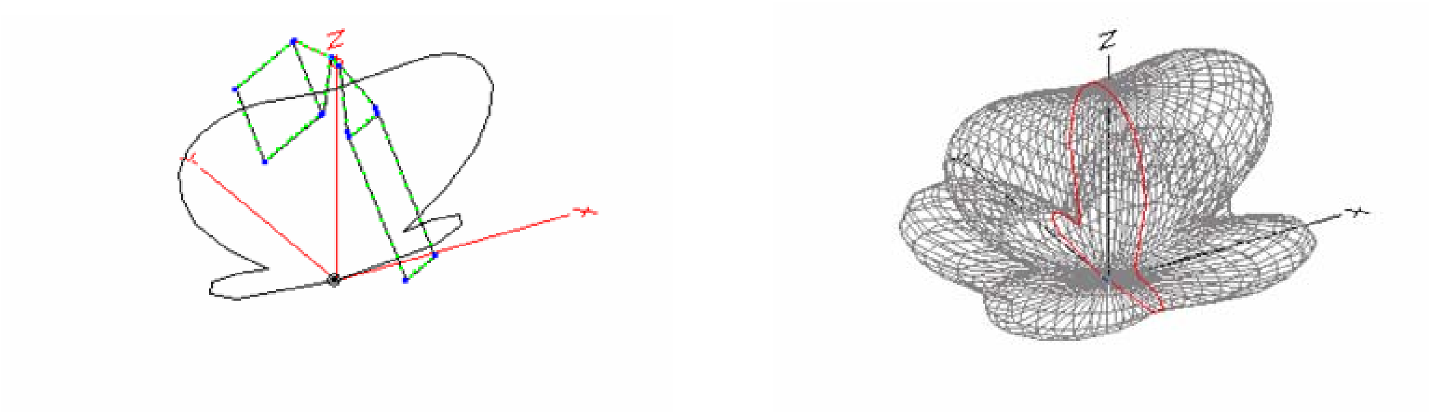

Figure 27. NLTA dipole, 90 MHz: HPBW = 40° E-plane, 101° H-plane.

The VSWR graph, Figure 28, shows the $\lambda/2$ and $3\lambda/2$ resonant frequencies for the NLTA dipoles. The fat dipole arms lower the VSWR somewhat, compared to the ASTRON design, throughout the frequency range.

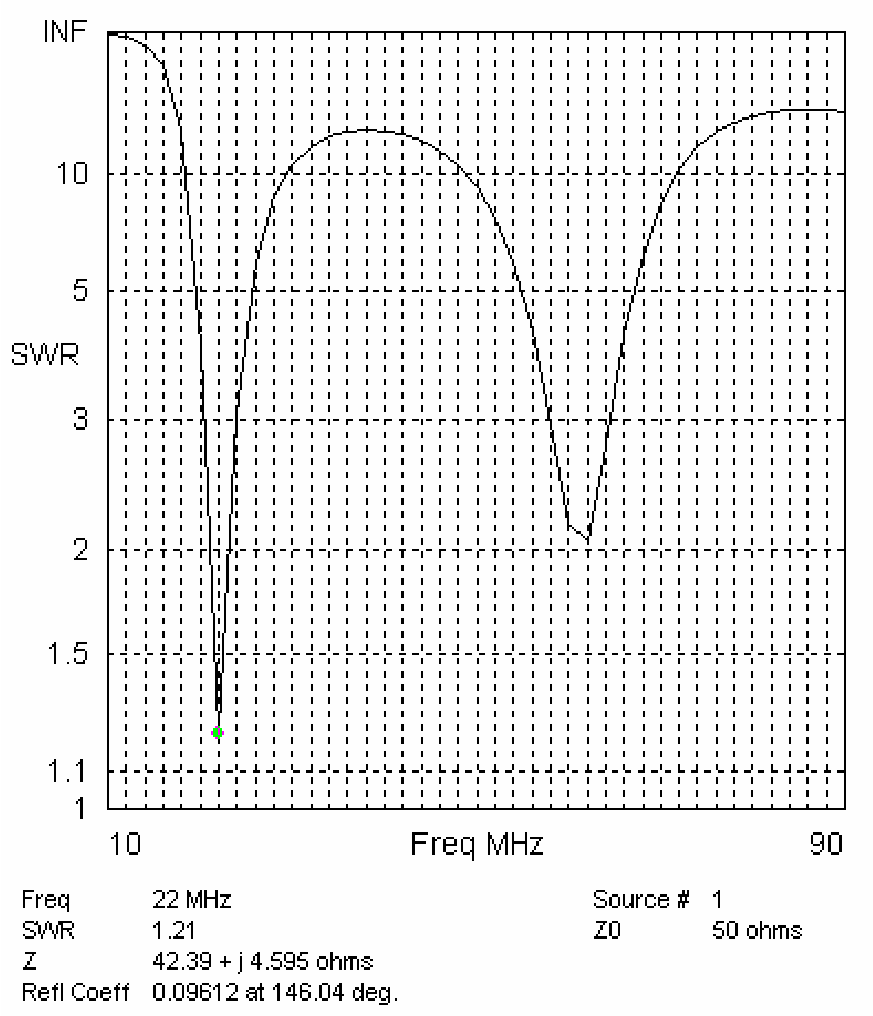

Figure 28. VSWR of the NLTA antennas in a 50 Ω feed line.

4.4 Zigzag Log-Periodic

The form of these zigzag antennas can be specified entirely in terms of angles and, apart from the need to limit the size, not by any dimension. Its properties are therefore independent of frequency within these limits. The low-frequency performance is limited by the practical need to terminate the structure at a finite size. The high-frequency limit is determined by the fabrication accuracy of the smallest zigzags. The constant wire diameter of 3 mm assumed in these simulations violates this rule, but it does not destroy the approximate frequency independence as long as the wavelength is much greater than the wire diameter.

Figure 29 through Figure 37 show the response patterns for a zigzag antenna with a vertex angle of 20°, a scale ratio of 0.9, and a height of 12 m. The base is 5 m square. Although these figures do not show it, this design can easily be made sensitive to dual polarizations by adding two more zigzags rotated 90° about the z-axis from the ones shown. The HPBW is much less than the LOFAR specification of 120º. Although it is easy to modify this design to increase the directivity (decrease HPBW), so far we have not been able to increase the beam width significantly without destroying the frequency-independent properties of the antenna.

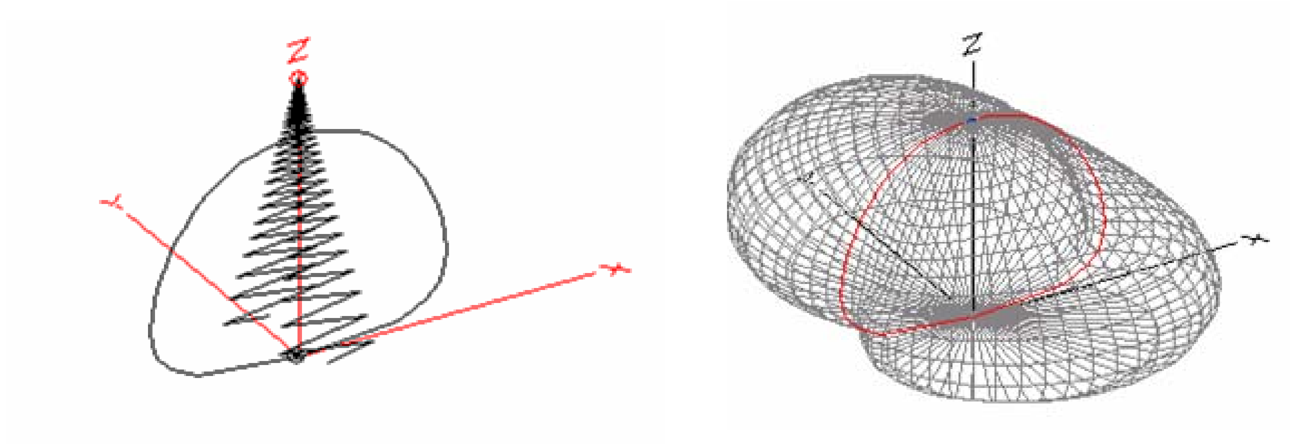

Figure 29. Zigzag pattern, 10 MHz: HPBW = 83° E-plane, indeterminate° H-plane.

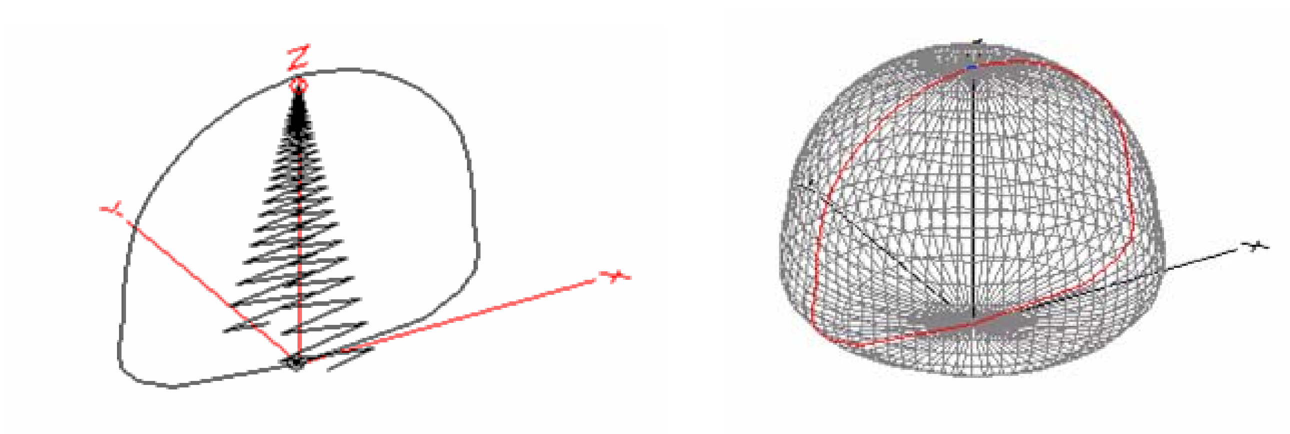

Figure 30. Zigzag pattern, 20 MHz: HPBW = 82° E-plane, 85° H-plane.

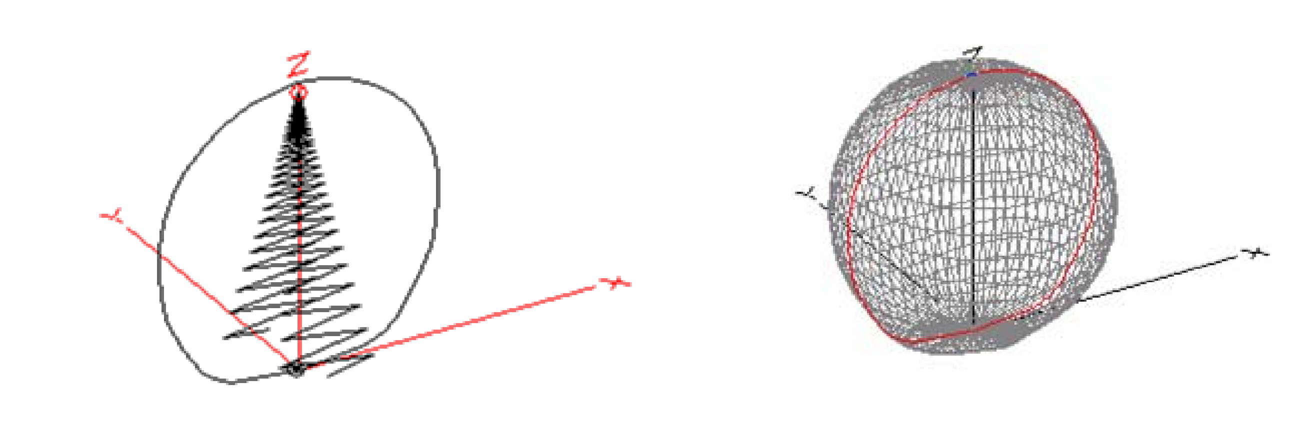

Figure 31. Zigzag pattern, 30 MHz: HPBW = 60° E-plane, 56° H-plane.

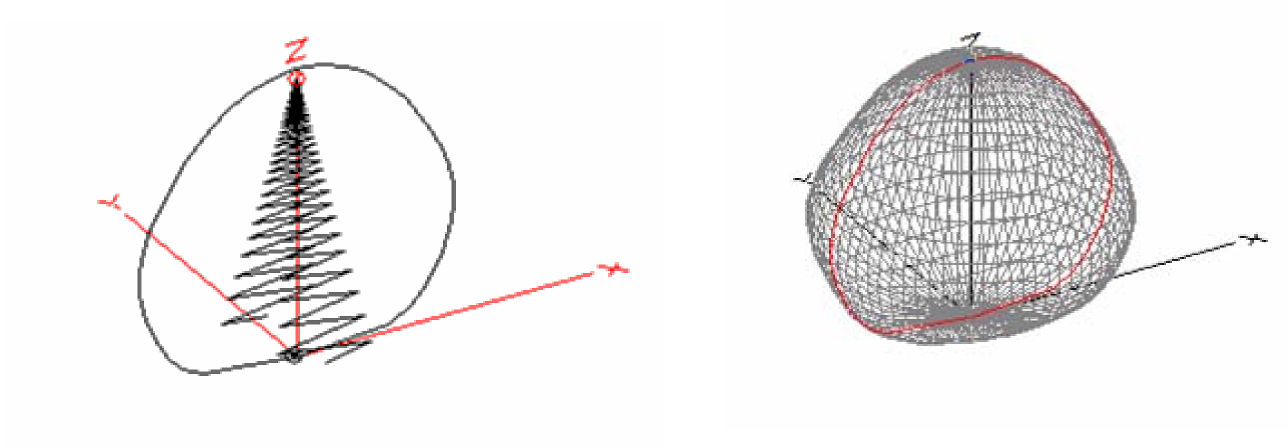

Figure 32. Zigzag pattern, 40 MHz: HPBW = 58° E-plane, 49° H-plane.

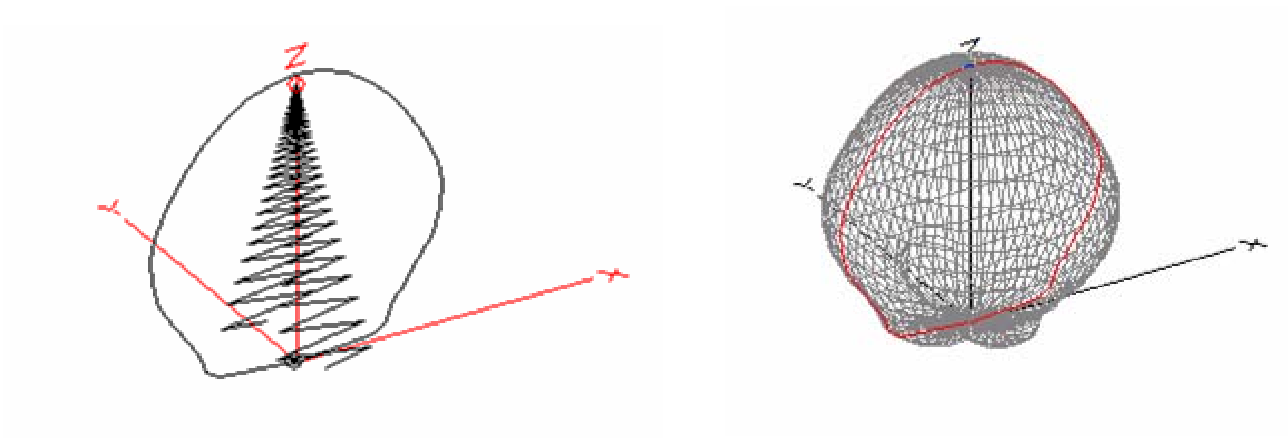

Figure 33. Zigzag pattern, 50 MHz: HPBW = 54° E-plane, 47° H-plane.

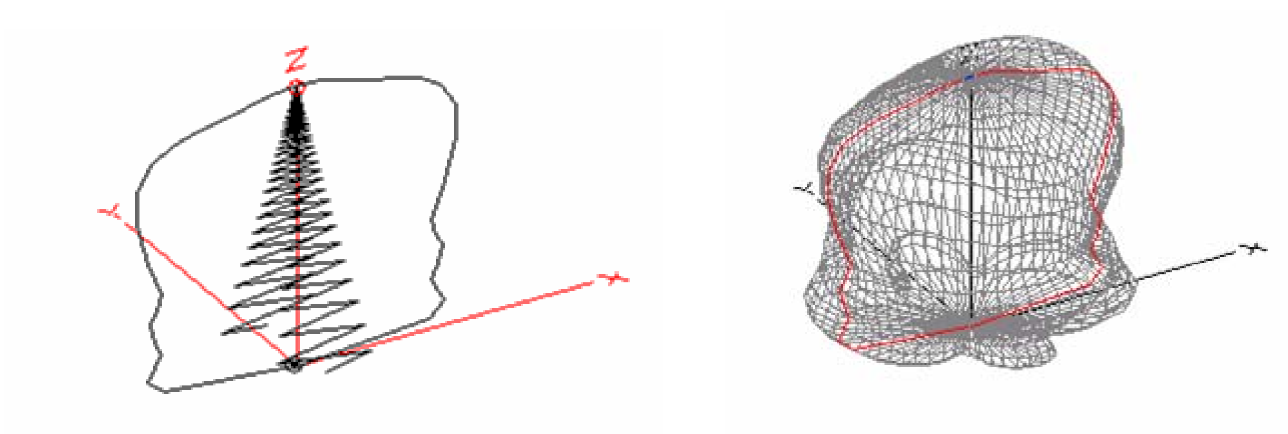

Figure 34. Zigzag pattern, 60 MHz: HPBW = 81° E-plane, 69° H-plane.

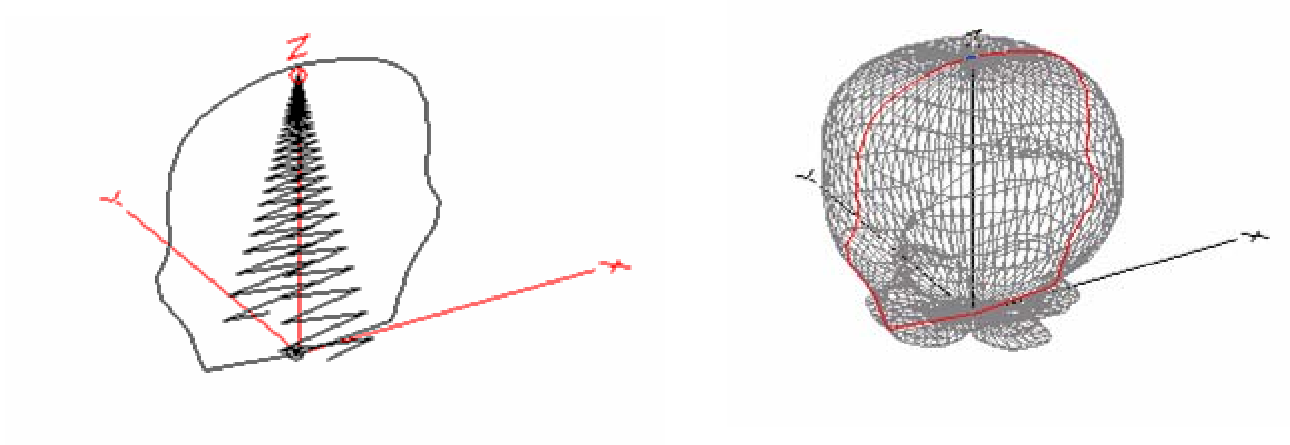

Figure 35. Zigzag pattern, 70 MHz: HPBW = 62° E-plane, 61° H-plane.

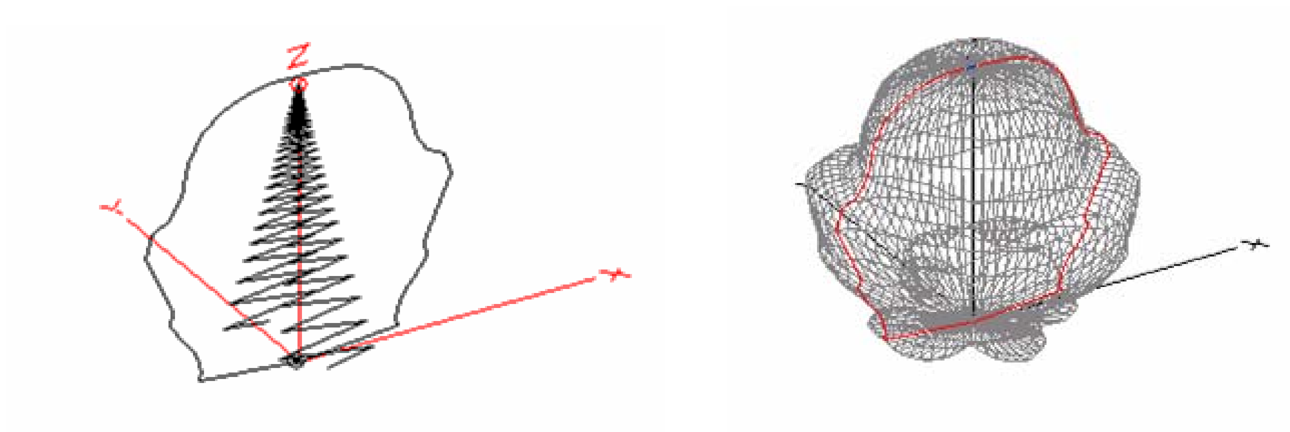

Figure 36. Zigzag pattern, 80 MHz: HPBW = 54° E-plane, 53° H-plane.

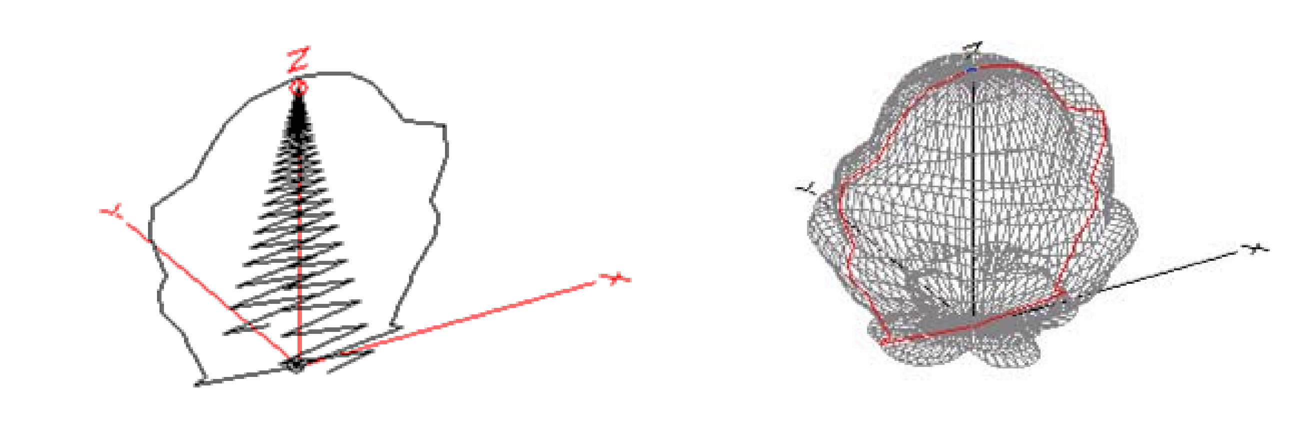

Figure 37. Zigzag pattern, 90 MHz: HPBW = 54° E-plane, 53° H-plane.

Figure 38 shows that, as expected, the feedpoint impedance of the zigzag is approximately independent of frequency for wavelengths shorter than twice the length of the base of the antenna. The feedpoint impedance predicted by these simulations is close to the theoretical value of 189 Ω for a self-complimentary log periodic antenna. A 200 Ω transmission line gives an approximate impedance match, and therefore a low VSWR, over a broad frequency range.

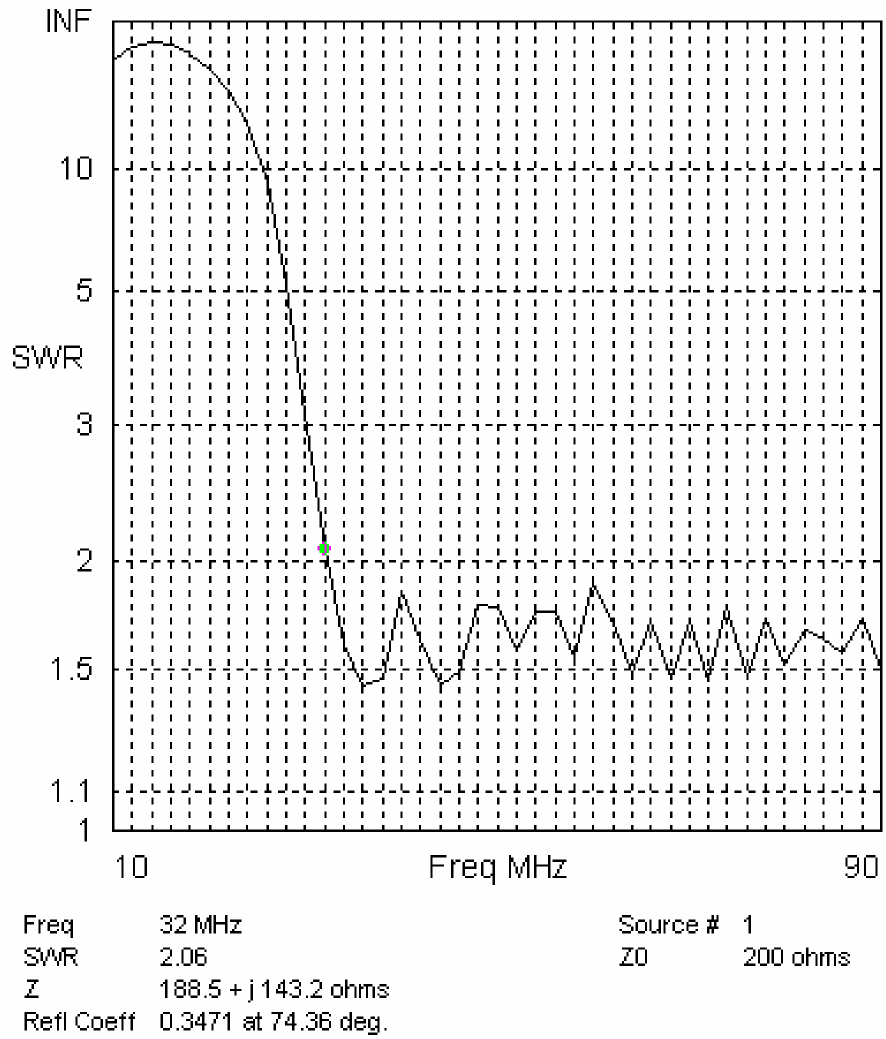

Figure 38. VSWR of zigzag antenna in a 200 Ω feedline.

4.5 Clark Lake/Nançay Conical Log Spiral

Conical log spiral or teepee antennas were used at the Clark Lake Radio Observatory (CLRO) and are currently in use in the Nançay Decameter Array (NDA) and at the University of Florida for solar and planetary observations. These antennas are approximately 7.2 m high and 5 m in diameter with a cone half-angle of 16° and are used from 10 MHz to 125 MHz. The ideal antenna would have two metal stripes spiraling on the surface of the cone, with their width equal to the distance between them giving a self-complementary structure. Each metal sheet was replaced by three wires, one along each edge and one along the center in order to simplify construction and decrease wind resistance. The antennas at these observatories all have two additional wires, which allow phase delays in steps of 45° by using diode switches to select which six wires are active at any time. This will not be necessary for LOFAR, which will use digital phase delays, so these simulations use six-wire models. We are also investigating the performance of two- and four-wire models.

The previous antennas also use load resistors at the ends of the wires to improve the SWR at the longest wavelengths. Although not included in the pattern results shown here, subsequent simulations confirm this observation.

The main disadvantage of spiral antennas is that they are sensitive only to one circular polarization component. Future work will investigate whether it is possible to design a counter wound, dual polarized version with adequate isolation between the two components. The HPBW of ~90º is also too narrow for LOFAR. Published results (Mayes, 1993, pp 9-85 – 9-88) indicate that it is possible to decrease the directivity by increasing the cone angle or increasing the spiral angle.

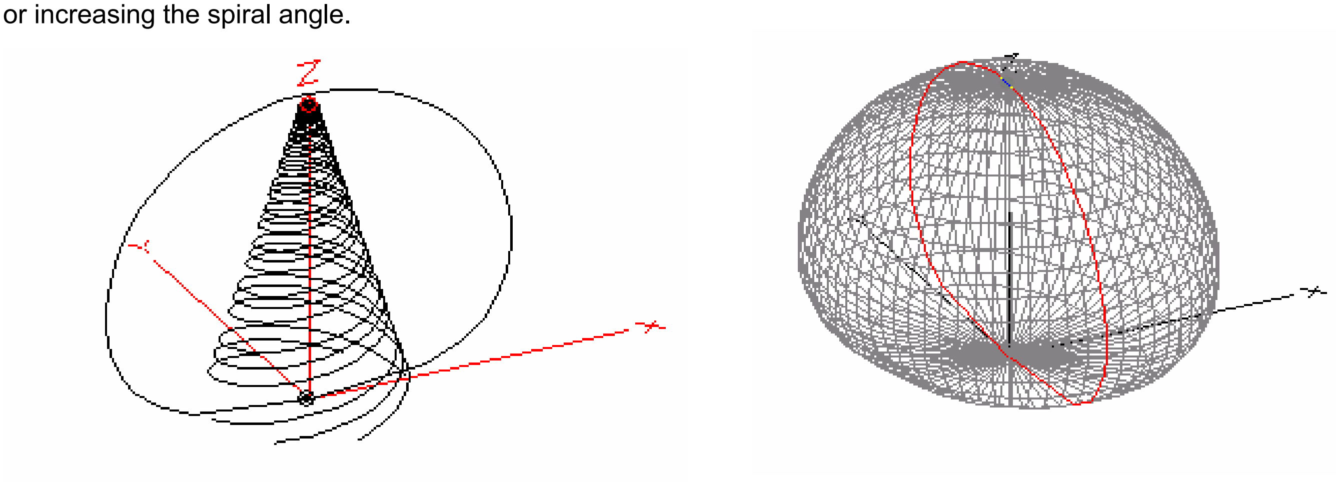

Figure 39. Conical log spiral response pattern, 10 MHz: HPBW = 91° E-plane, 111° H-plane.

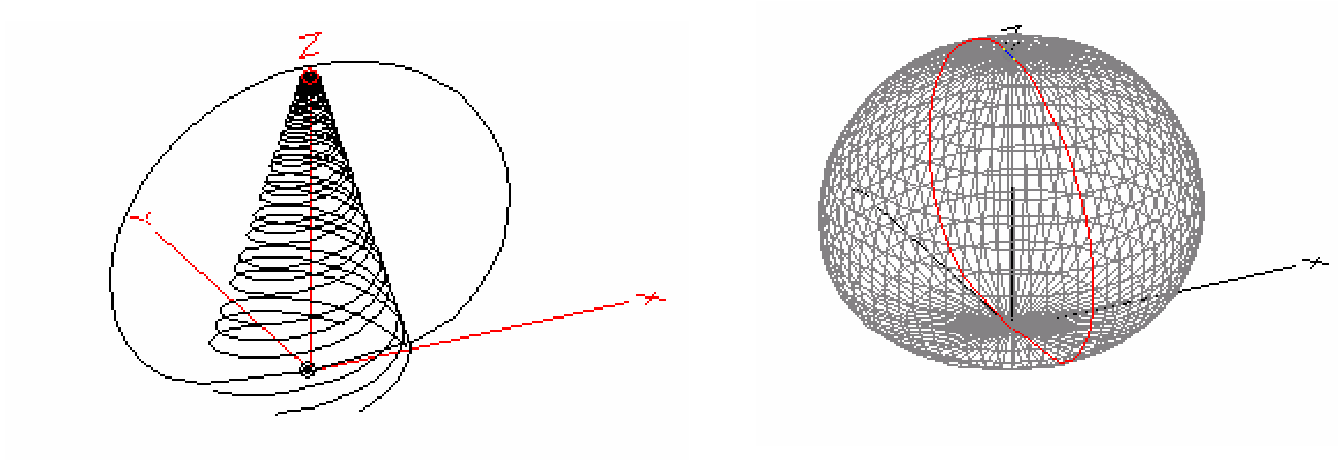

Figure 40. Conical log spiral response pattern, 20 MHz: HPBW = 90° E-plane, 81° H-plane.

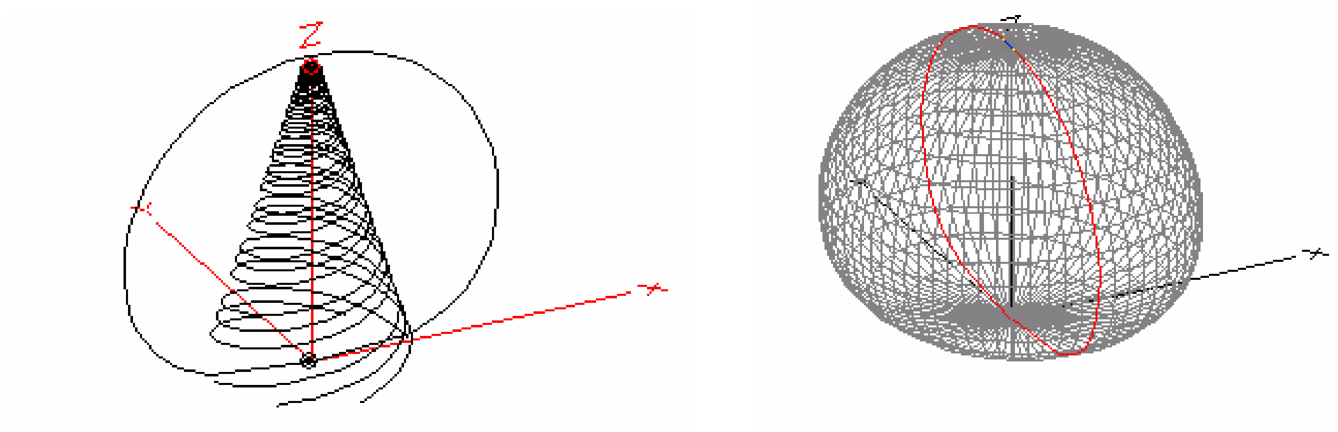

Figure 41. Conical log spiral response pattern, 30 MHz: HPBW = 79° E-plane, 94° H-plane.

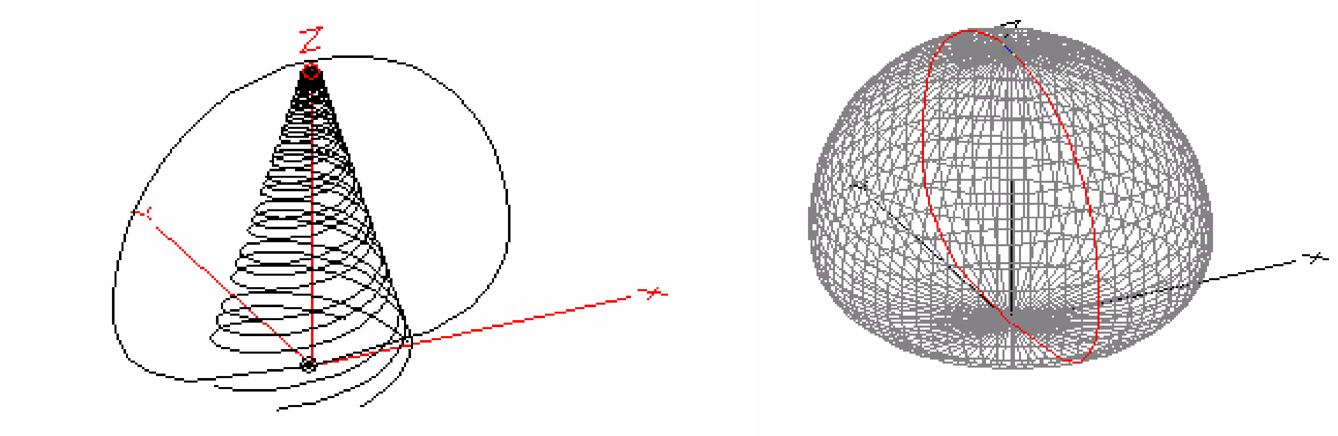

Figure 42. Conical log spiral response pattern, 40 MHz: HPBW = 80° E-plane, 94° H-plane.

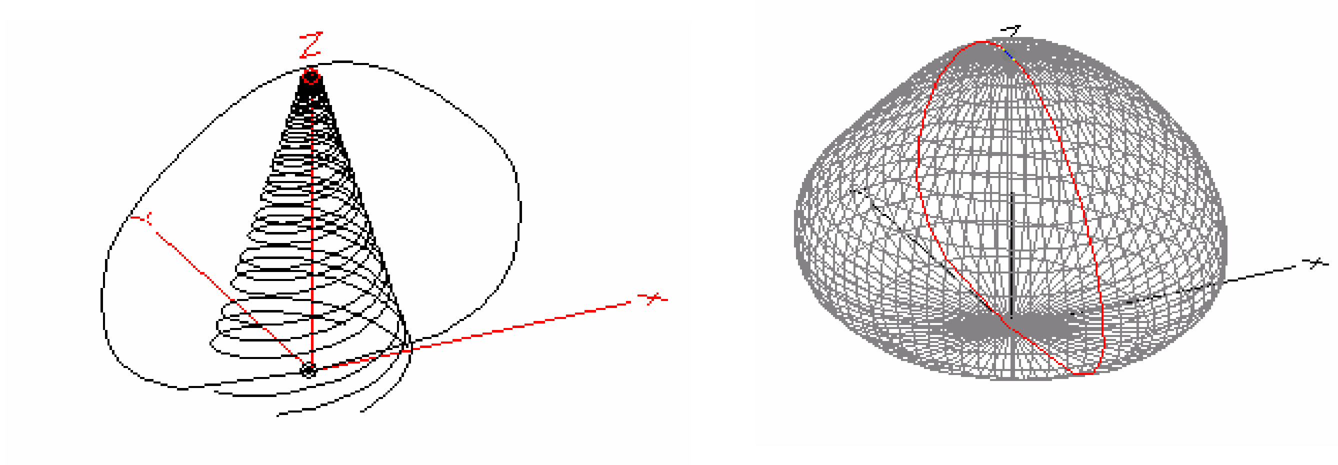

Figure 43. Conical log spiral response pattern, 50 MHz: HPBW = 92° E-plane, 80° H-plane.

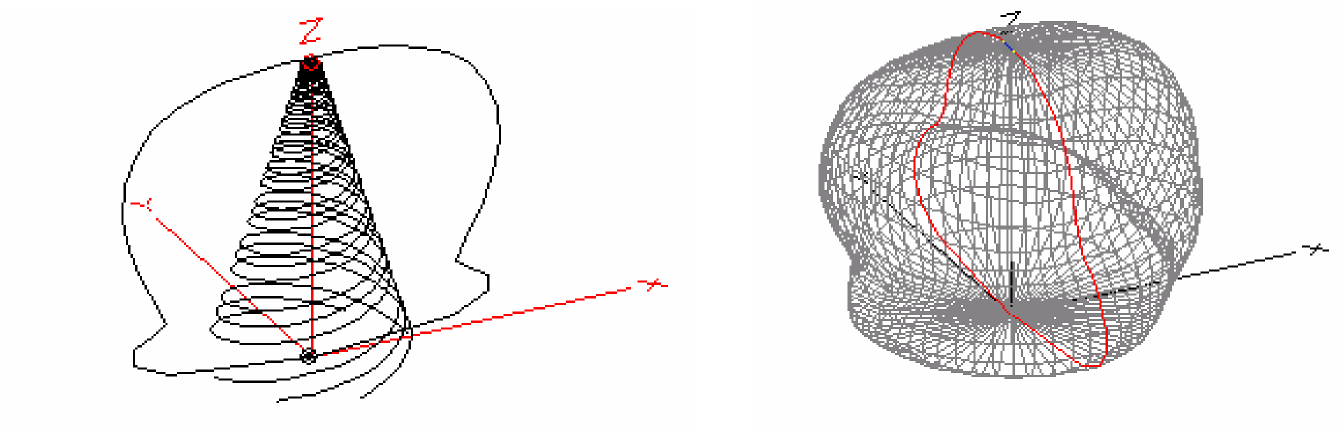

Figure 44. Conical log spiral response pattern, 60 MHz: HPBW = 88° E-plane, 63° H-plane.

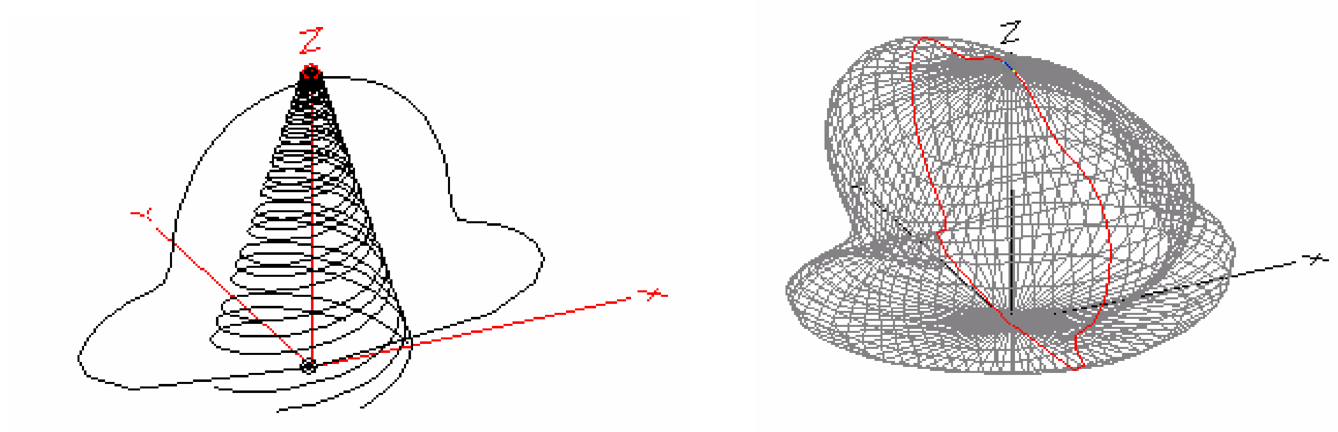

Figure 45. Conical log spiral response pattern, 70 MHz: HPBW =114° E-plane, 58° H-plane.

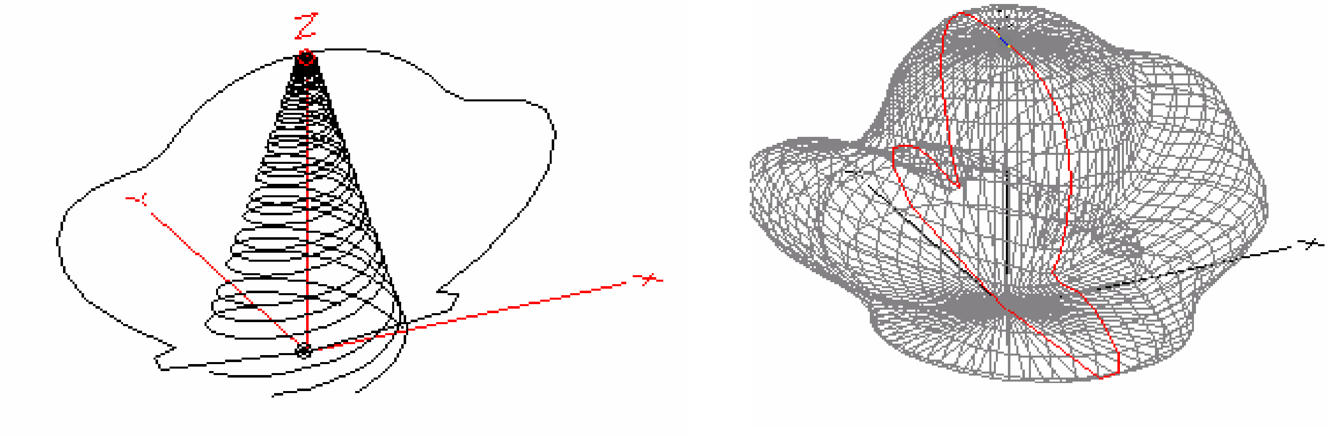

Figure 46. Conical log spiral response pattern, 80 MHz: HPBW =124° E-plane, 63° H-plane.

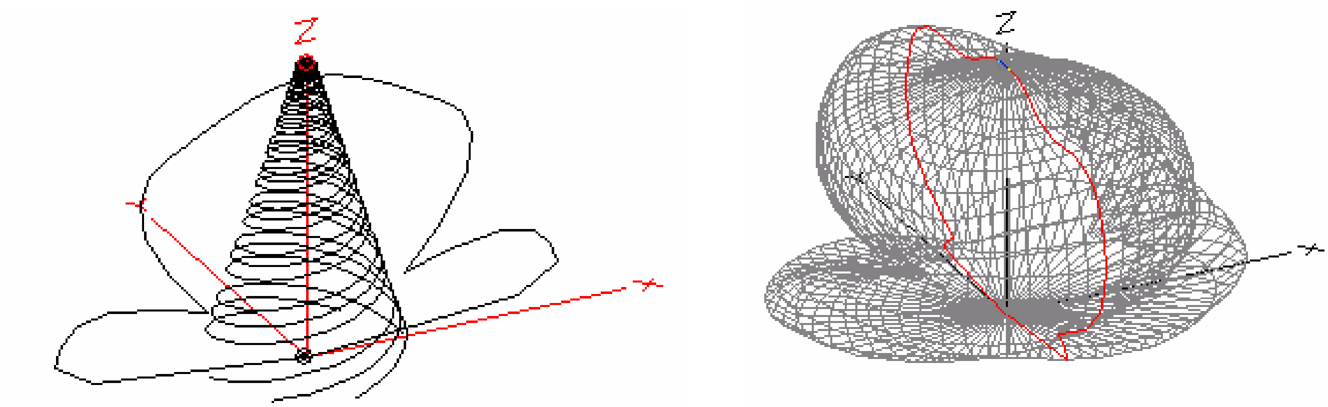

Figure 47. Conical log spiral response pattern, 90 MHz: HPBW = 84° E-plane, 118° H-plane.

Figure 48 shows that the VSWR of this frequency-independent design remains low over a very broad bandwidth. The characteristic impedance of the feedline is chosen to match the feedpoint impedance of the antenna. The apparent increase in VSWR at low frequencies is due to limitations in the ground plane simulation algorithms, which become inaccurate when antenna wires are within a small fraction of the wavelength of the ground. Both theory and experiment (W. C. Erickson, private communication) indicate that the VSWR goes to 1:1 in the low frequency limit.

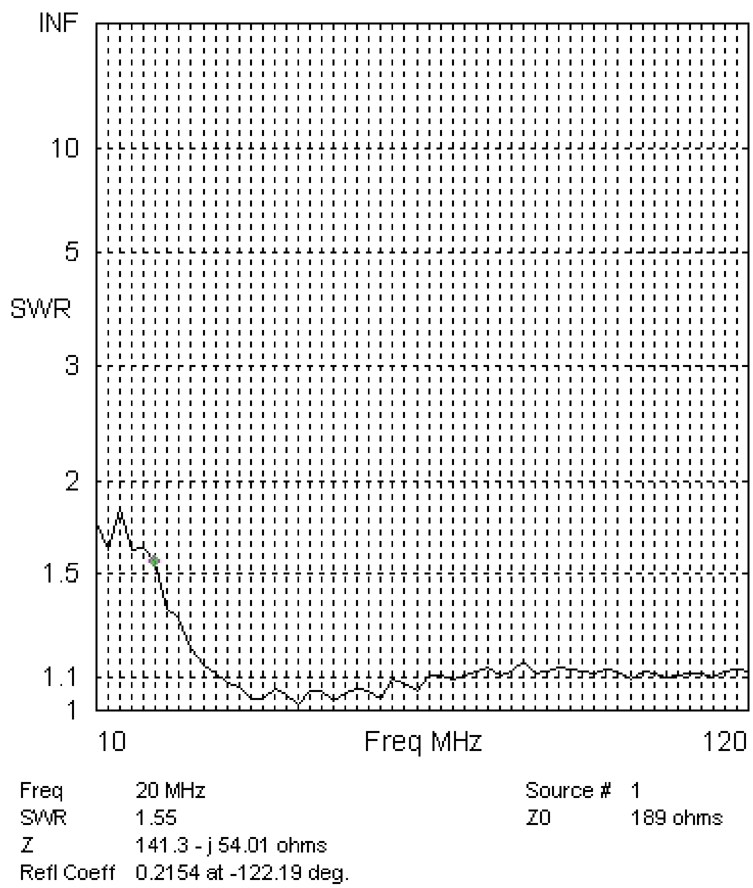

Figure 48. VSWR of a terminated conical log spiral in a 189 Ω feedline.

4.6 Sinuous Antenna

The sinuous antenna is another example of a self-complimentary log periodic design. The design shown below (Figure 49) is sensitive to two orthogonal polarization components, either linear or circular. In the planar configuration it is bidirectional, but like the log spiral, it can be made unidirectional by mapping it onto the surface of a cone. Absorbing material placed beneath the antenna is another possibility. Figure 50 shows the response pattern at 40 MHz of a 5 m diameter sinuous antenna.

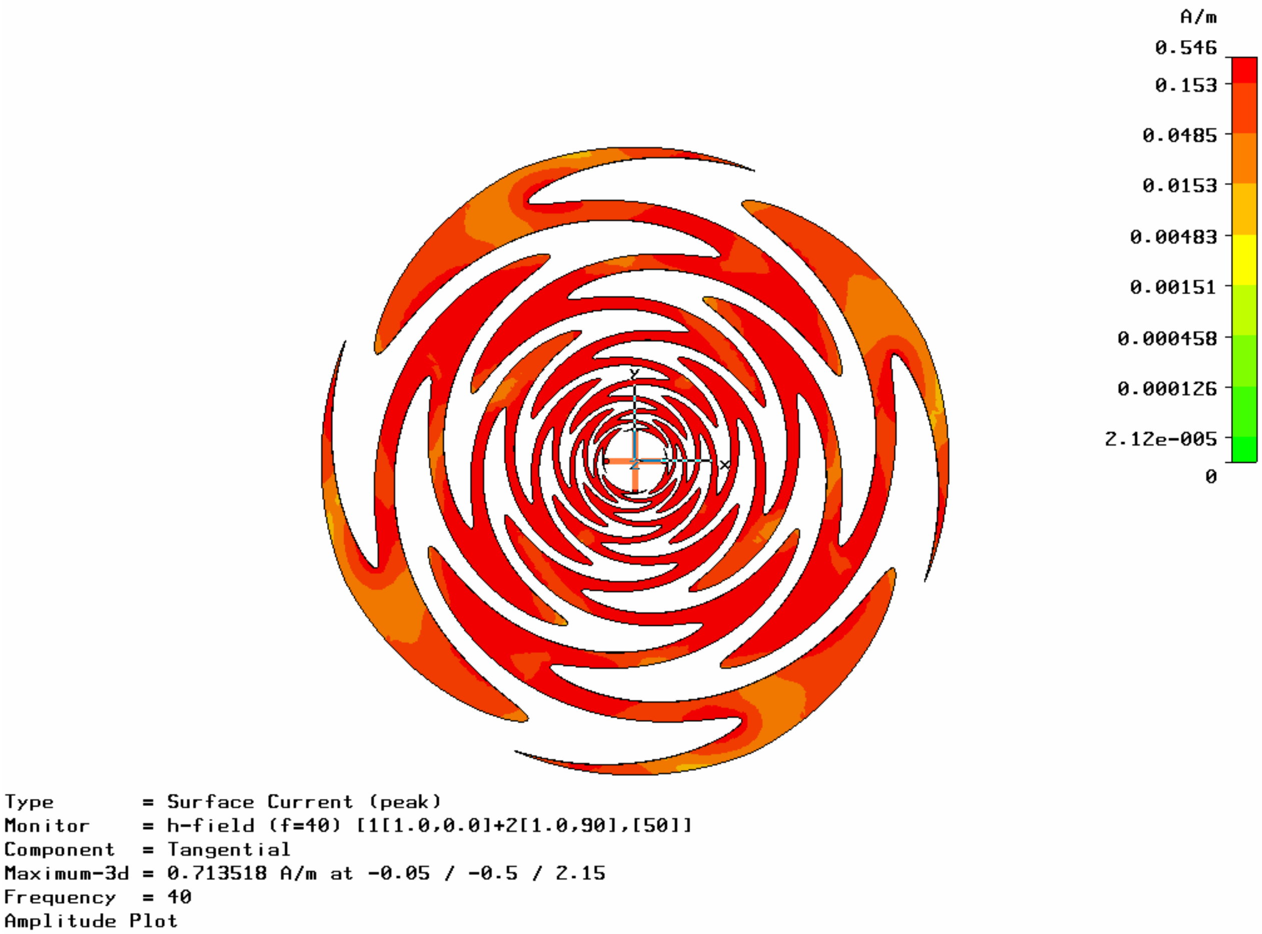

Figure 49. Surface currents in a sinuous antenna, calculated by CST Microwave Studio.

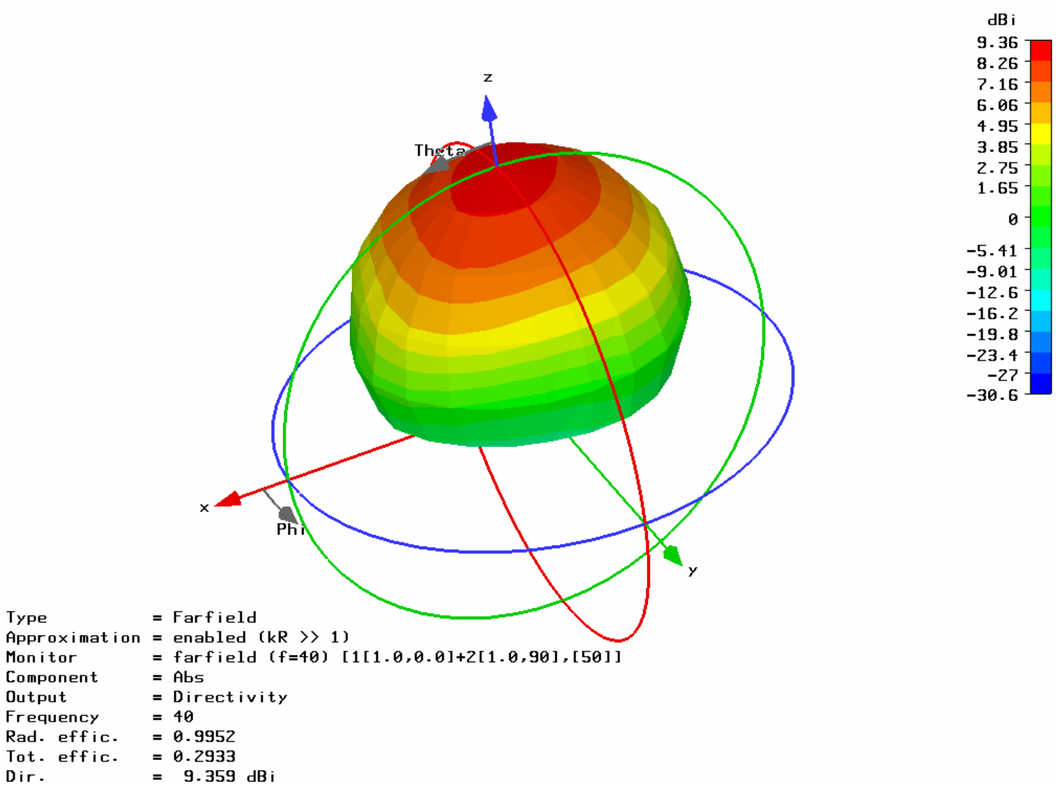

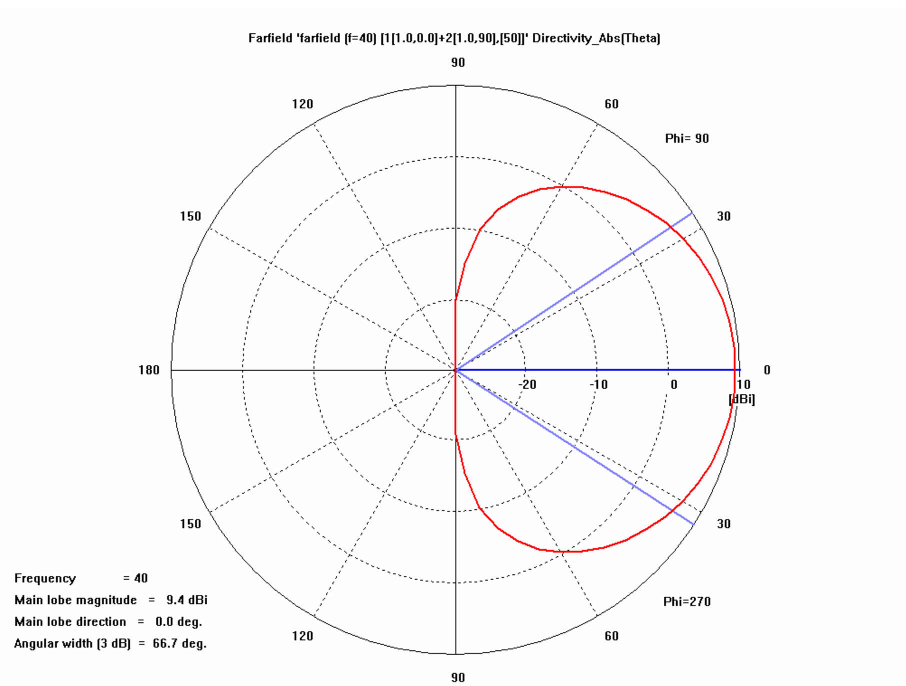

Figure 50. 3D and 2D response pattern of the sinuous antenna.

4.7 Ground Plane Issues

Although probably not important for the unidirectional zigzag and teepee designs, the active dipoles may require a conductive ground screen beneath each antenna to decrease losses due to the finite soil conductivity and to minimize weather-induced changes in antenna response. In order to assess the importance of a ground screen, we repeated the NLTA simulations using a reasonable range of values for the dielectric constant and conductivity of the soil in the high-accuracy Sommerfeld model for an infinite, homogeneous ground plane. Table 2 and Figure 51 show that for soil parameters from the extremes of dry, sandy desert to rich farmland, the gain of the antennas changes < 3 dB at 10 MHz, < 1 dB at 30 MHz, and even less at higher frequencies.

These calculations imply that a ground screen is not needed to remove the effects of weather-induced changes in soil properties provided that variations in antenna response of at most 2 – 3 dB can be corrected by calibration techniques during data collection/reduction. In the absence of a ground screen the absolute gain decreases due to increased losses at low frequencies as the height of the antenna decreases relative to the wavelength. This may be acceptable because the Galactic background is very bright at these frequencies.

Table 2. Parameters used in the ground plane calculations and their effect on antenna gain.

Relative Quality	Dielectric Constant	Conductivity (S/m)	Maximum Gain (NLTA: 30 MHz) dBi	Maximum Gain (NLTA: 10 MHz) dBi
Poor	10	0.002	3.5	-1.1
Average	13	0.005	3.7	-0.6
Very Good	20	0.030	4.3	1.7
Salt Water	80	5	5.7	6.3
Perfect	—	∞	5.9	7.1

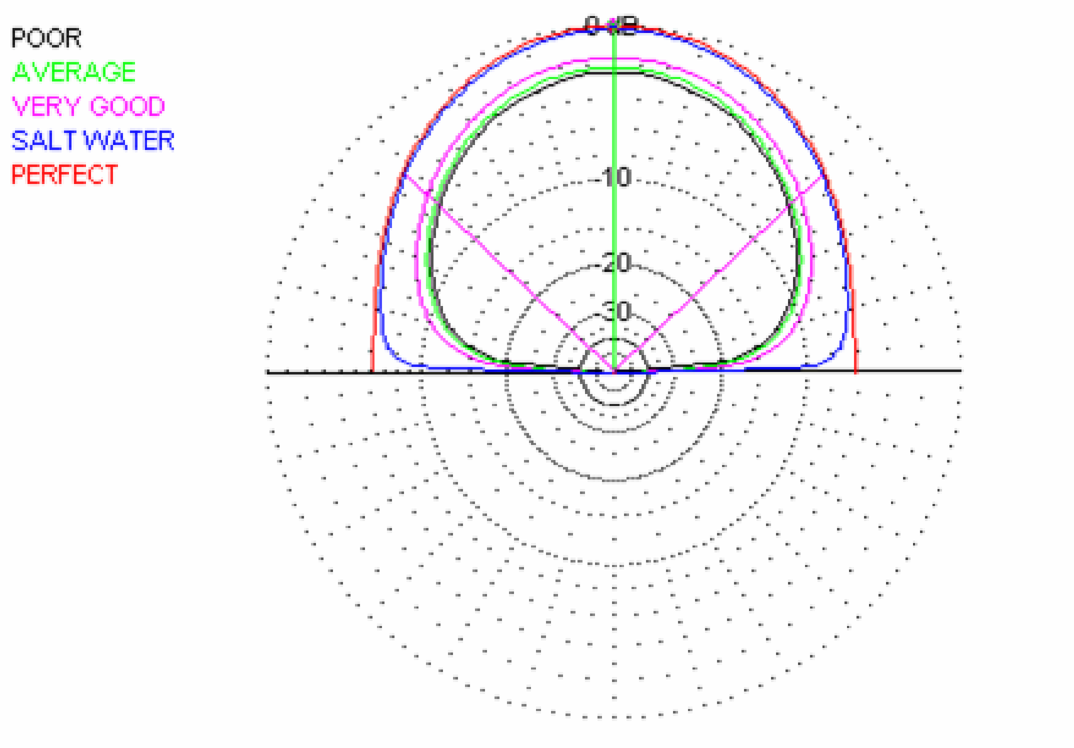

Figure 51. Calculated response patterns at 30 MHz showing the effects of varying soil conditions.

4.8 Summary of Antenna Characteristics

Table 3 shows our attempt at a relative assessment of the suitability of various antenna designs for use in LOFAR. Log periodic antennas generally have narrower beamwidths than active dipoles, but they vary less with frequency, and are more nearly equal in the E and H planes. All of the designs can detect orthogonal polarization components except for the conical log spirals, which are sensitive only to one circular component, depending on which way they are wound. Ground screens would be a significant expense, but these simulations indicate that response variations due to changing ground conditions are small and could be corrected by calibrations.

Table 3. Summary of antenna properties.

	Beam-width	E-H plane Difference.	Dual Polarization	Ground Screen	Feedpoint Impedance	Cost
Baseline (ASTRON)	80º – 130º	10º – 40º	Yes	Maybe	R: 4 – 1300 Ω X: -1500 – +1300 Ω	$
NLTA	40º – 140º	10º – 90º	Yes	Maybe	R: 10 – 700 Ω X: -400 – +400 Ω	$$$
Clark Lake/ Nançay	80º – 120º	10º – 40º	No	No	Nearly const. ~190 Ω	$$?
Zigzag	50º – 80º	0º – 15º	Yes	No	Nearly const. ~190 Ω	$$
Sinuous	~70º	~0º	Yes	Yes	Nearly const. ~190 Ω	$$$$

5 Summary and Plans for Future Development

There has been great progress in the development of the active-balun subsystem required for LOFAR, ASTRON, NRL, and NRAO have formed a cooperative association that has explored a wide variety of existing designs and methodologies. Together, we are rapidly converging on a solution that is specifically suited to the cost and performance requirements of LOFAR. Three prototype designs have been constructed and tested in both the laboratory and the field. The performance of these designs is sufficiently close to achieving target specifications that the risk previously associated with this subsystem has been considerably reduced. It is also encouraging to note that all of the existing designs are presently being employed in scientific experiments in an operational capacity (THETA, LOPES, ITS, NLTA, NASA-GDRT, and BIRS). It is reasonable to expect that a final design leveraging the strengths of all of these designs will soon be completed and then optimized for mass production and integration into the LOFAR prototyping.

6 References

H. V Cane, Mon. Not. R. Astron. Soc. **189**, 465 (1979).
R. H. DuHamel and J. P. Scherer in *Antenna Engineering Handbook,* edited by Richard C. Johnson (McGraw-Hill, New York, 1993) Chap. 14.
Paul E. Mayes in *Antenna Handbook,* edited by Y. T. Lo and S. W. Lee (Van Nostrand Reinhold, New York, 1993), Vol. 2, Chap. 9.